Synthesis of Nanomaterials

Mohammad Jafarzadeh
Faculty of Chemistry, Razi University

Dekker Encyclopedia of Nanoscience and Nanotechnology,

By Schwarz, J. A., Contescu, C. I., Putyera, K. (Editors); Marcel Dekker: New York, 2004.

3. Fabrication of Nanoarchitectures Using Lithographic Techniques

Two major approaches can be taken: non-lithographic and lithographic methodologies.

Non-lithographic methods include a mix-and-grow procedure or using exchange reactions. Nanodomains of organic thin film materials have been produced by mixing desired components in solution (or vapor), then soaking solid substrates in the mixture.

Similar nanodomains may be obtained by immersing a pure thin film in a solution containing another adsorbate.

The domain sizes and distribution are determined by the interplay of surface reaction kinetics and thermodynamics.

In contrast to non-lithographic methods, the nanostructures produced using lithographic approaches are not at the mercy of thermodynamics and kinetics. Instead, the features are determined by the designs of lithographic masks, or by the trajectory of the probes.

The word lithography is generally used in the context of microelectronics where structures are defined in semiconductor wafers like Si or GaAs to make devices. Such a definition of lithography however refers to the top-down approach.

In the context of fabrication of nanostructures one needs to broaden the definition of lithography to include bottom-up routes that are often employed to synthesize nanostructures or their arrays. In this route of lithography, the created pattern either directs the growth process or constrains the growth to within a nanometer or few tens of nanometers.

Nanolithography also includes a mask for conventional dry or wet etching, as in conventional lithography albeit using novel routes.

Nanomanipulation is intimately related to nanolithography. This is an enabling tool for assembly and manipulation of nanosized objects like nanoparticles, nanotubes and nanowires.

Methods of microfabrication include photolithography and micromachining, and also electron- and ion-beam lithography, and microcontact printing (µCP) have broken the wavelength barrier to produce patterns as small as 300 nm.

To distinguish between micro and nanolithography, techniques that are capable of producing feature sizes of 100 nm or smaller refer to nanolithography.

In optical lithography, short wavelengths have been employed, such as deep UV (F_2 laser with h= 157 nm) and extreme UV lithography (EUV, with radiation of 134 nm).

For further miniaturization, soft X-ray (h= 0.5-4 nm), electron-beam and ion-beam-based lithography have come into play which utilize masks or focused beams.

Less expensive approaches include nonconventional lithographies such as nanoimprint and microcontact printing.

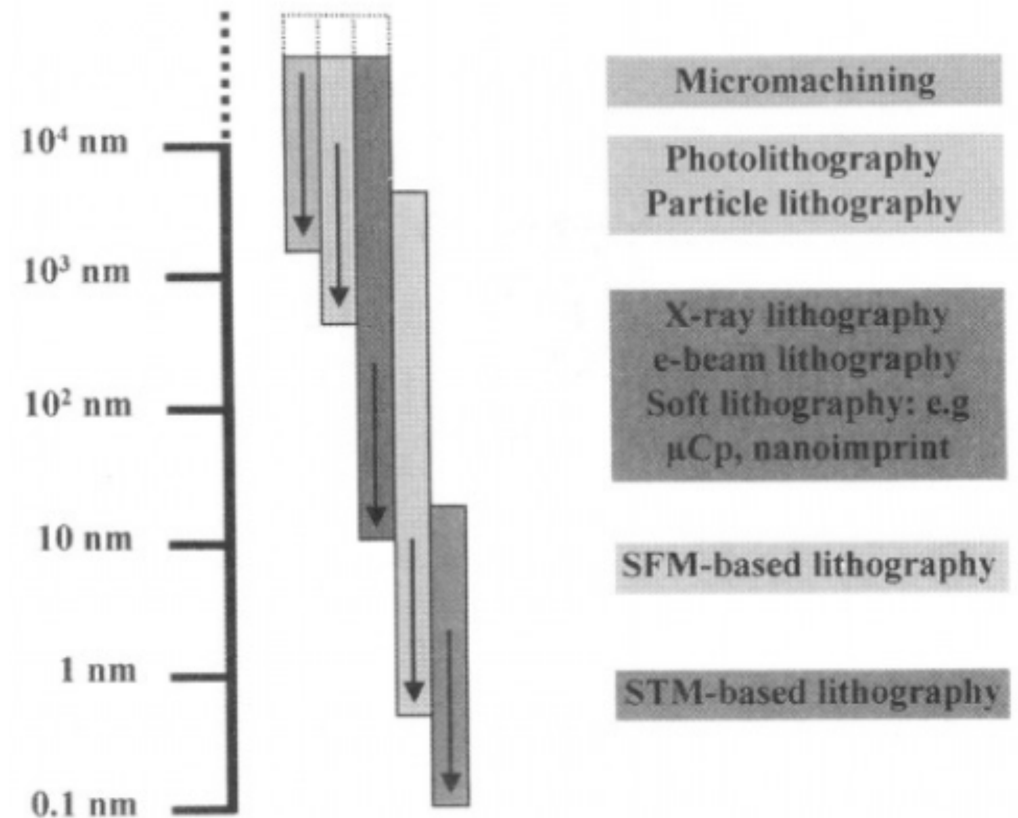

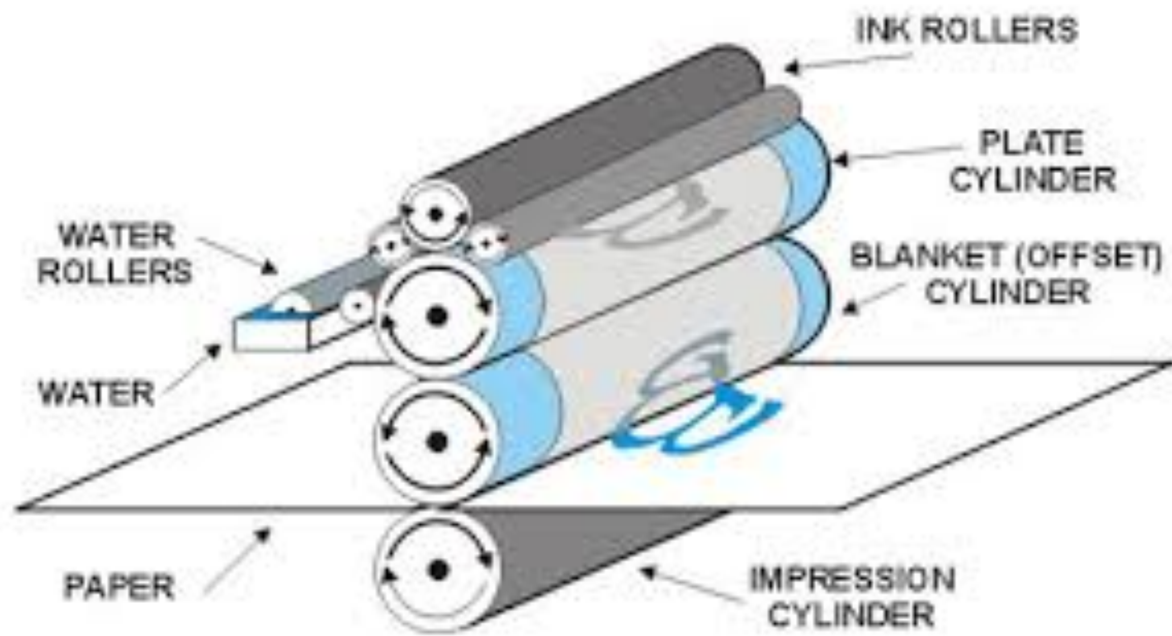

a. Prepare wafer

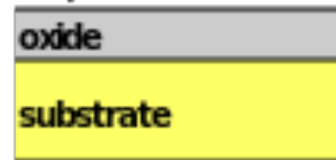

b. Apply photoresist

c. Align photomask

d. Expose to UV light

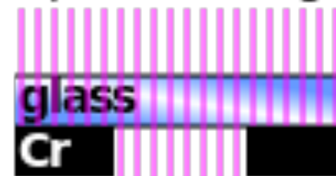

e. Develop and remove photoresist exposed to UV light

f. Etch exposed oxide

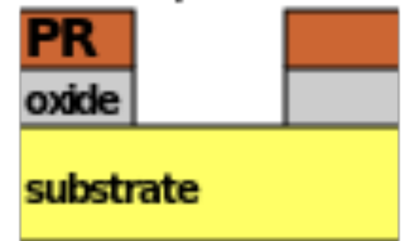

g. Remove remaining photoresist

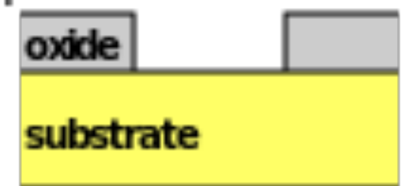

X-Ray Lithography

In conventional photolithography, a projection configuration is used, where a collimated light passes through a mask and illuminates the resist surfaces. Depending on the optics used, various magnifications may be projected onto the resists.

There are no ideal materials available for X-ray projection. Therefore, shadow mask techniques were developed, which consist of a thin membrane of SiC, Si_3N_4, or Si, and heavy metals such as Ta, W, or Au to absorb X-ray photons. These masks are produced using microfabrication/processing and electron-beam lithography.

Frequently used X-ray sources include synchrotron X-ray or laser-induced plasma sources. The resolution of proximity X-ray lithography is limited by the Fresnel diffraction and by the scattering of photoelectrons in the resist materials such as polymethylmethacrylate (PMMA).

At present, standard X-ray lithography has produced features as small as 70 nm, while phase-shifting masks have reached 40-70 nm region.

Soft X-ray is capable of exposing relatively thick resists with a high aspect ratio. PMMA resists with submicron features and 100 μm depth are reported. Although X-ray lithography is still at the research stage, many researchers predict that it is the most promising tool in meeting the high spatial precision and high throughput criteria of manufacturers.

Electron- and Ion-Beam Lithography

In electron-beam lithography, a focused electron-beam may be achieved by converting a commercial SEM or TEM instruments, which operate at 50–100 kV. The electron-beam has very high energy, and is focused on a tiny spot (a few nanometers).

The spot can be moved by the electron optics following a programmed trajectory.

The resolution is not determined by the spot size, but rather by electron scattering, which impacts both the exposed and nearby areas (proximity effect).

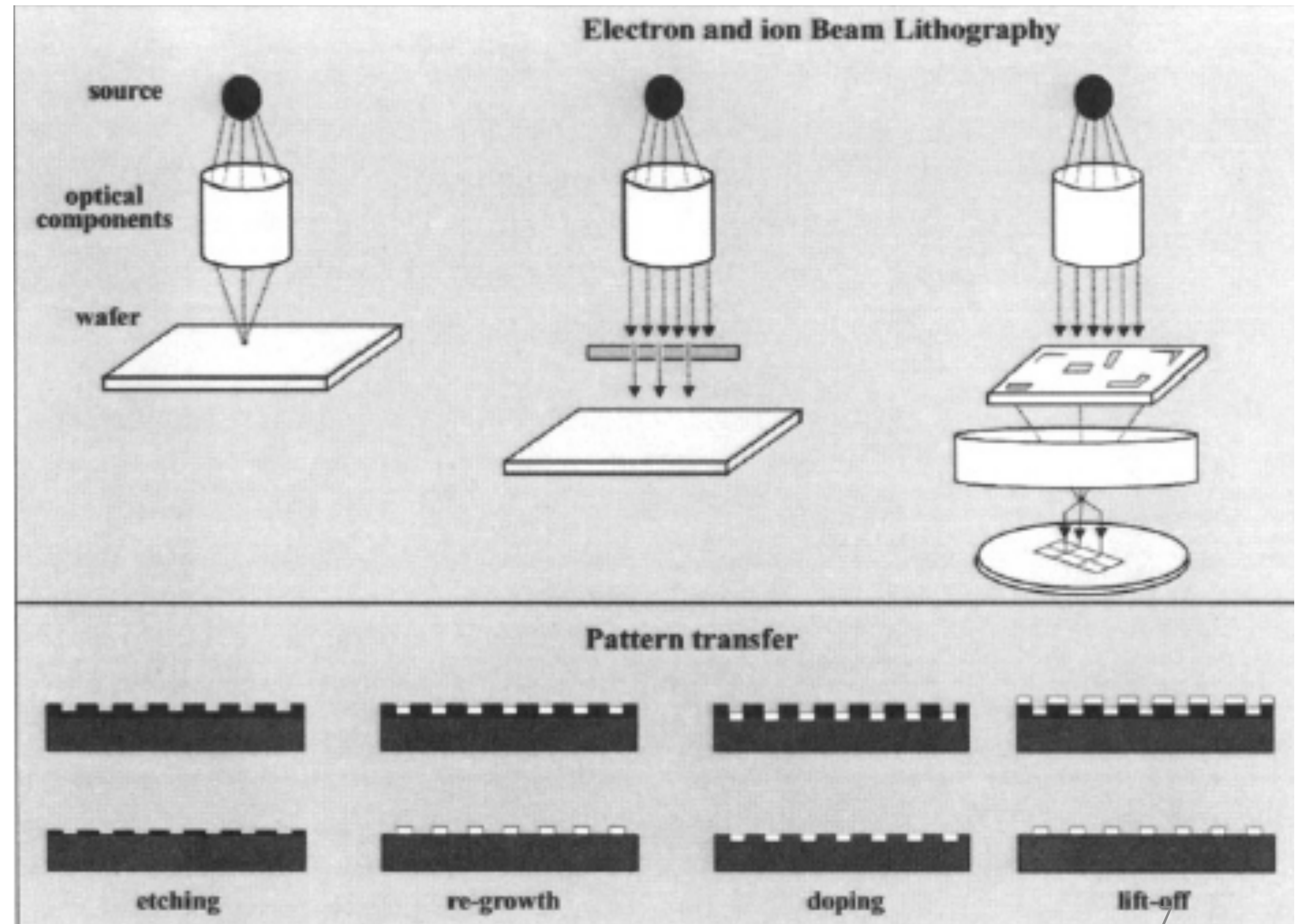

The advantages of this configuration include bypassing masks, and the simplicity in employing home-designed features.

The shortcoming is its serial nature, that results in low throughput.

Electron-beam lithography with focused electron-beams has been widely employed to produce masks that are used for X-ray lithography and nonconventional lithography such as microcontact printing and nanoimprint. In addition, electron-beams are also used for hole drilling, and for surface modification of various inorganic materials as well as organic thin films.

The focused beam configuration can also be applied to ion-beam lithography, where beam of positive ions (instead of negatively charged electrons) such as H^+ or He^+ are produced by plasma ionization of gas molecules, and then extraction of ions. The ions may be focused by electrostatic lens to a “point.”

Analogous to electron-beam lithography, the ions may be moved by ion optics following a programmed trajectory. Resolution and speed are similar to electron-beam lithography, although ion-beams suffer far less scattering effect.

Taking advantage of the high resolution (20 nm) and high energy (up to hundreds of kilo eV), focused ion-beam is used in the integrated circuit (IC) industry to ion mill transistors and contacts.

For manufacturing IC, high throughput is required. Parallel approaches are used which involve the use of masks. In masked ion-beam lithography, a mask (often a 1X stencil mask) is posted in close proximity to the resist, while a well-collimated ion-beam illuminates the resist surface through the mask to transfer the feature to the resist coatings.

Typical ion energies range from 70 to 150 keV. For high-resolution applications, ion-projection lithography is used.

Ion optical components are adopted after the ions pass through the mask to form a reduced image on the resist. Stencil masks utilize single crystal Si membranes (2.5 µm thickness) since mask fabrication may be achieved using in the standard Si processing procedures.

At present, a 100 nm feature size with less than 10 nm distortion can be reached using commercial setups.

NANOPARTICLE LITHOGRAPHY

To produce periodic arrays of nanostructures, a relatively inexpensive and simple method of NP (or nanosphere) lithography has attracted much attention.

Monodispersed latex particles are simple to synthesize and purify. For particle lithography of inorganic materials, the procedures are illustrated in Fig. 6.4. Particles can assemble into ordered, and closely packed 2D and 3D structures under carefully controlled conditions. These assemblies are used as templates, where the void space is filled with the materials of interest. Particles can then be removed by either calcination or solvent dissolution.

Arrays of nanostructures are produced, which include 2D and 3D arrays of metals, metal oxides and silica, porous membranes of polyurethane, as well as 3D opal or reversed opal structures of photonic band-gap materials such as SiO_2 and TiO_2.

Similar methods may be adapted to produce 2D arrays of protein nanostructures. First the protein and latex are mixed to desired concentrations. The mixture is then deposited on the substrate and allowed to dry. Guided by the assembly of latex spheres, an ordered structure is formed, consisting of close-packed latex particles decorated by proteins in the void spaces. The latex template is then rinsed away with deionized water, resulting in periodic arrays of protein nanostructures on the substrate.

2-D or 3-D periodic arrays of inorganic materials

A. Preparation of a nanoparticle array

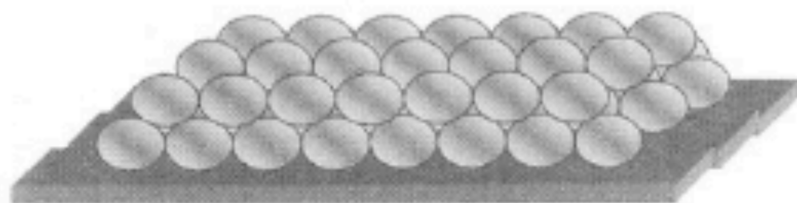

B. Deposition or intercalation of inorganic materials

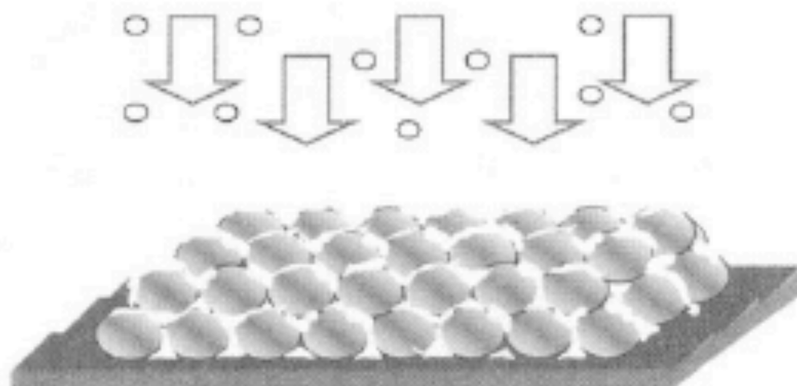

C. Removal of latex particles (by calcination or dissolution)

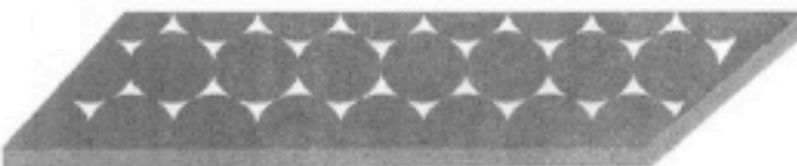

2-D periodic arrays of biomaterials

A. Mixing of latex particles and protein molecules

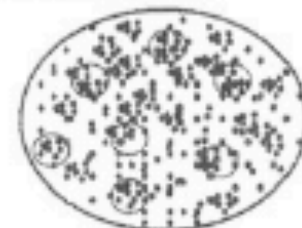

B. Deposition onto a flat surface

C. Drying and ordering of latex particles

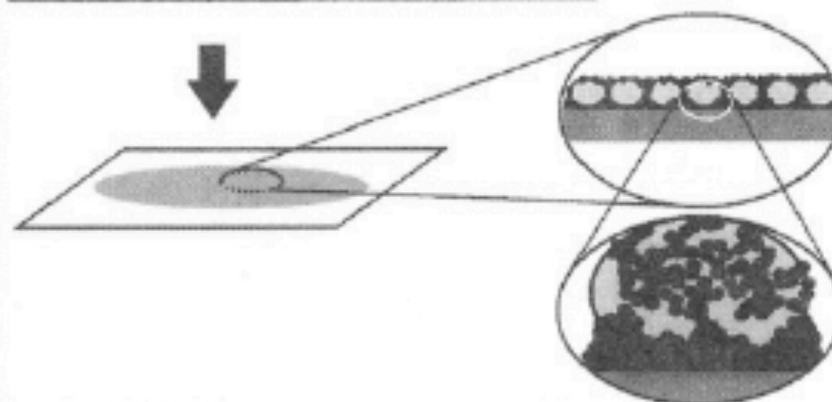

D. Removal of latex templates via rinsing

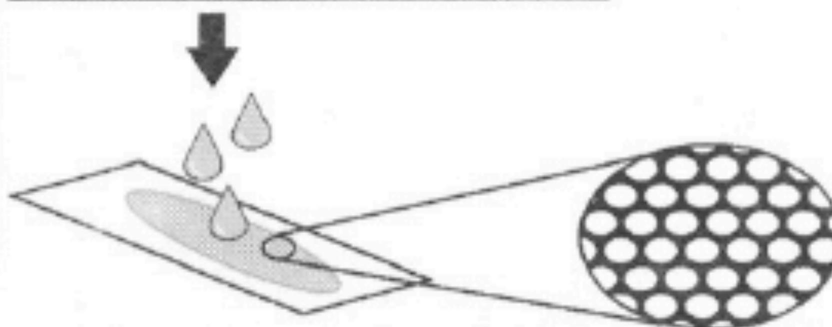

Periodic arrays of nanostructures of proteins have been successfully produced, e.g. the production of nanostructures of bovine serum albumin (BSA). The periodicity of the BSA nanoarrays is 206 nm.

Most protein molecules retain their activity because specific antibodies such as rabbit-anti-BSA immunoglobulin G (IgG) can bind to the adsorbed BSA particles.

Compared with X-ray, electron- and ion-beam lithography, nanosphere lithography is simpler and less expensive.

One can easily adapt this method to produce periodical nanoarrays in a research laboratory.

In comparison to scanning-probe lithography (SPL), NP lithography is able to produce nanostructures with higher throughput.

SCANNING PROBE LITHOGRAPHY

Resolution and Nanofabrication

Scanning probe microscopy such as STM and AFM are well known for their capability to visualize surfaces of materials with the highest spatial resolution.

In terms of structural characterizations, AFM can attain a lateral resolution of 0.1 Å and vertical resolution of 0.05 Å.

STM resolution is intrinsically five times higher than AFM. These high resolutions are reached for crystalline systems. For noncrystalline surfaces or soft-and-sticky surfaces, it is more difficult to achieve high resolution.

Despite the structural complexity of SAMs and macromolecules, high-resolution images have been obtained using both AFM and STM. In the case of an alkane-thiol SAM, defects such as steps, etch pits (gray spots) and single layer islands (bright spots) are clearly visible.

More importantly, the superlattice with respect to the basic structure was resolved for the first time using AFM. The periodicity and single molecular defects at the domain boundary of a SAM are also resolved.

In the case of immobilized proteins on a planar surface, individual lysozyme (LYZ) molecules are visible from the AFM topograph, from which the orientation of the proteins may be extracted. Detailed structural features of nonplanar and large biosystems, such as bacteria and cells, can also be revealed using AFM.

Taking advantage of the sharpness of the tips, and strong and localized tip–surface interactions, SPM has also been used to manipulate atoms on metal surfaces, and to fabricate nanopatterns of metal and semiconductor surfaces.

In principle, by enhancing these local interactions such as atomic force, density of tunneling electrons or electrical field strength, one should be able to break chemical bonds selectively.

Various approaches in controlling the local interactions to obtain sharp patterns with high spatial precision have been reported, which include: AFM-based lithography such as tip-catalyzed surface reactions, dip-pen nanolithography (DPN); and STM-based lithography such as single molecule manipulation, tip-assisted electrochemical etching and field-induced desorption.

SPL cannot produce large numbers of patterns as rapidly as photolithography or electron lithography, because of its unparalleled spatial precision and its capability to fabricate and image in situ.

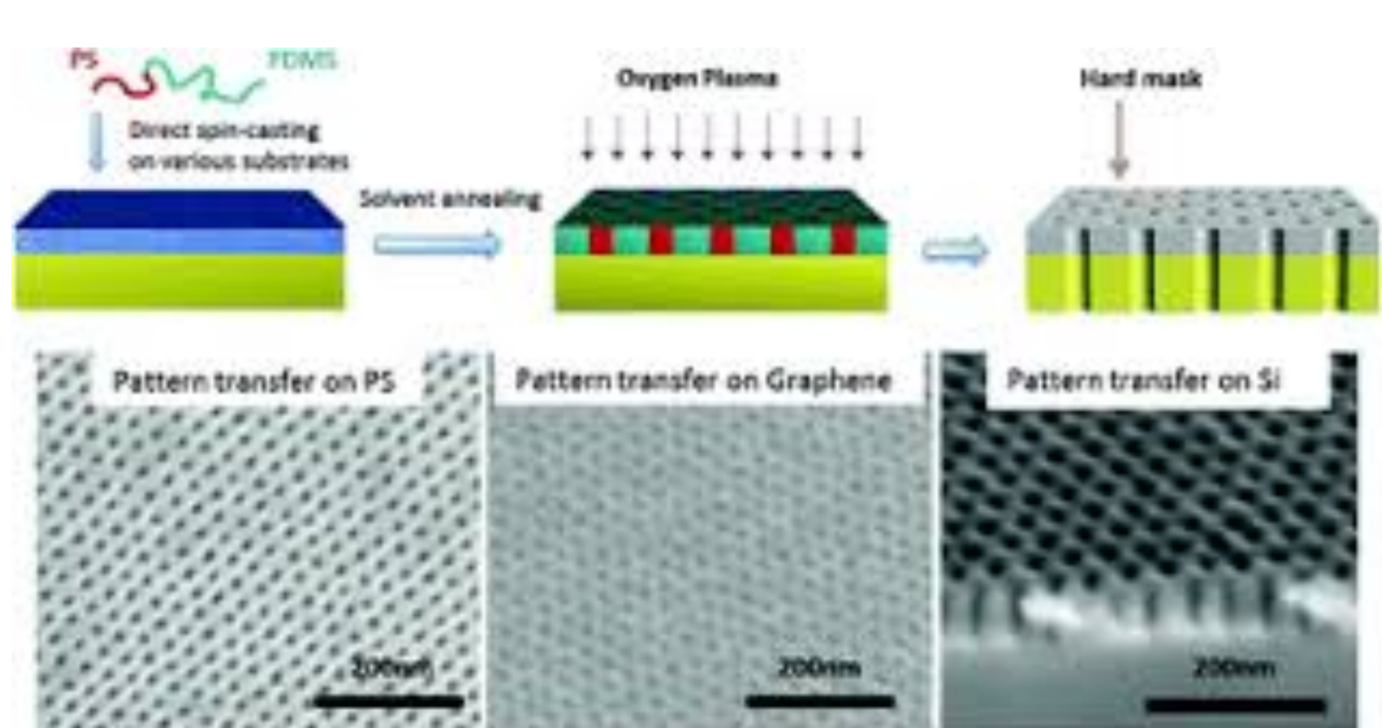
PS
PDMS
Direct spin-casting on various substrates
Solvent annealing
Oxygen Plasma
Hard mask
Pattern transfer on PS
Pattern transfer on Graphene
Pattern transfer on Si
200nm
200nm
200nm

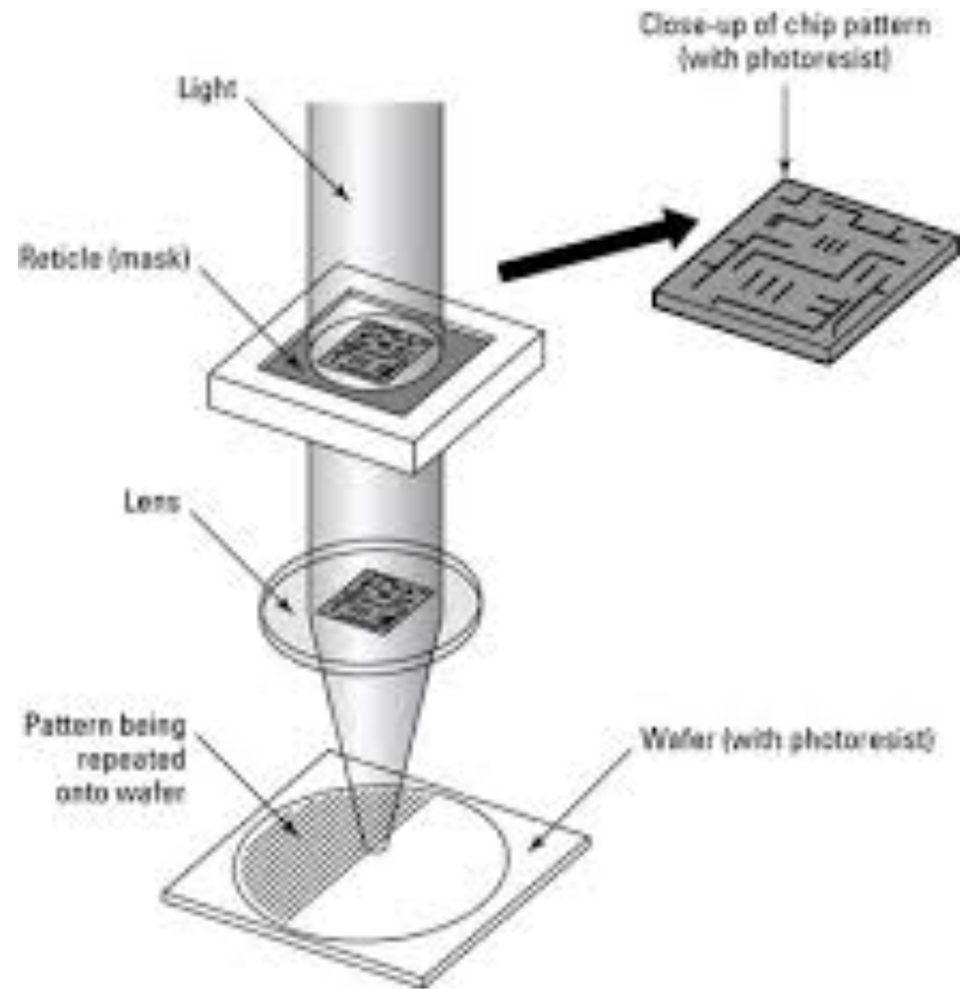
Light
Close-up of chip pattern (with photoresist)
Reticle (mask)
Lens
Pattern being repeated onto wafer
Wafer (with photoresist)

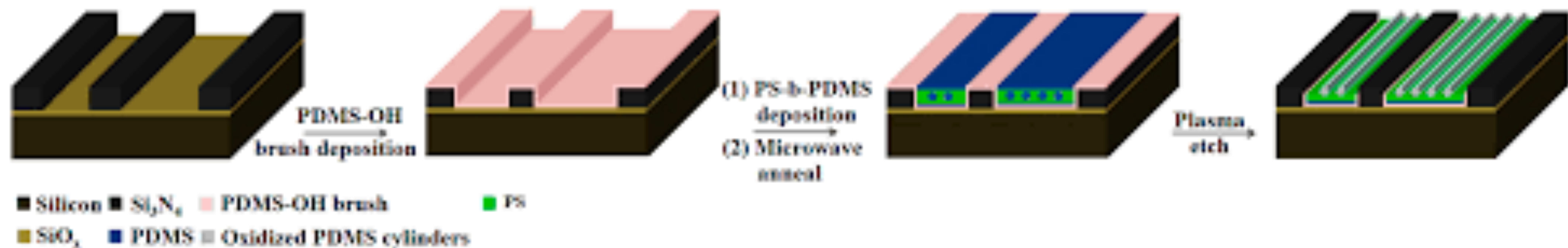
PDMS-OH brush deposition
(1) PS-b-PDMS deposition
(2) Microwave anneal
Plasma etch
Silicon
Si_3N_4
PDMS-OH brush
PS
SiO_x
PDMS
Oxidized PDMS cylinders

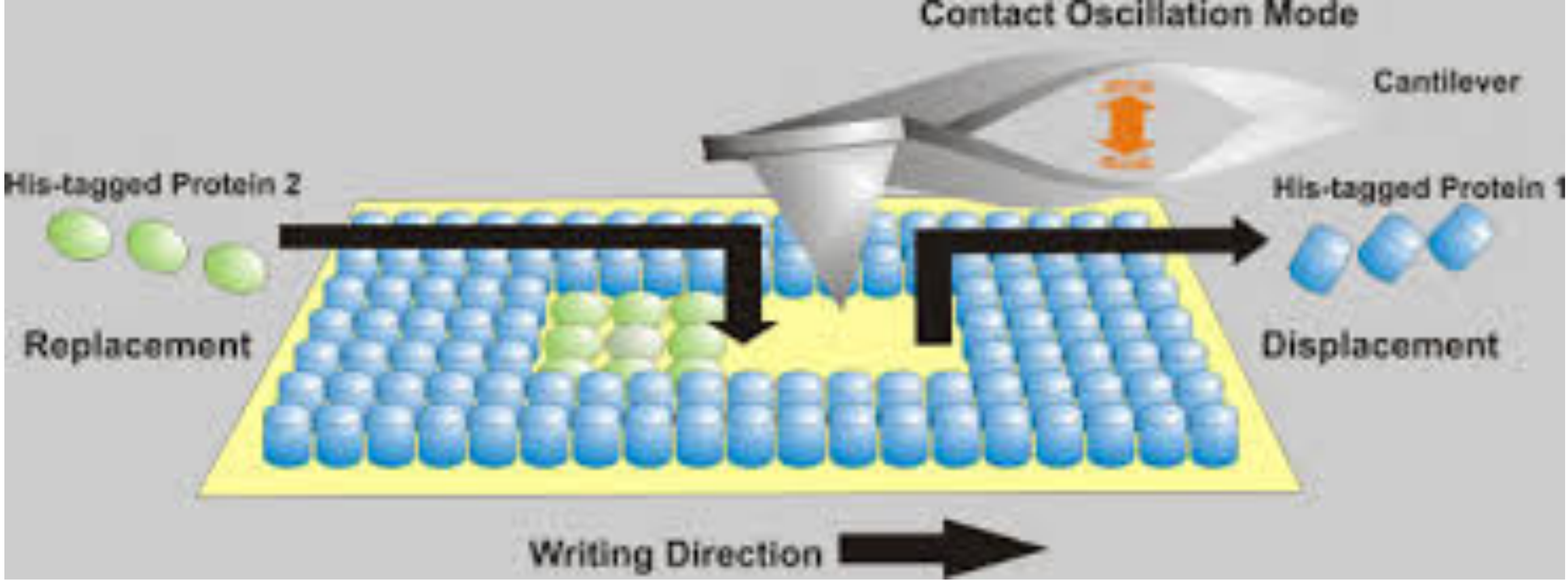

Contact Oscillation Mode
Cantilever
His-tagged Protein 2
His-tagged Protein 1
Replacement
Displacement
Writing Direction

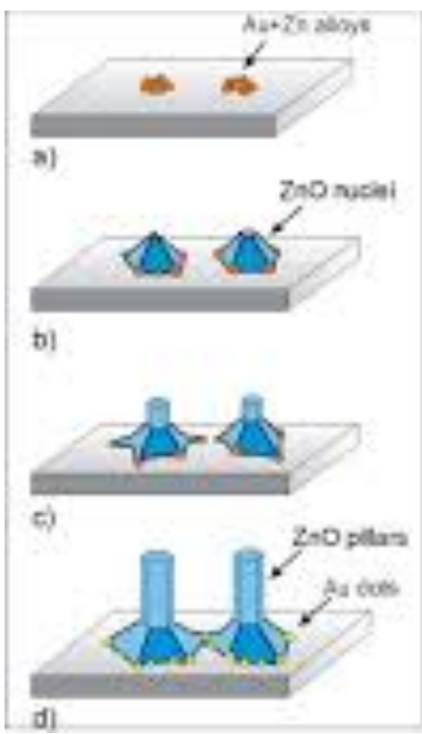

Au+Zn alloys
a)
ZnO nuclei
b)
c)
ZnO pillars
Au dots
d)

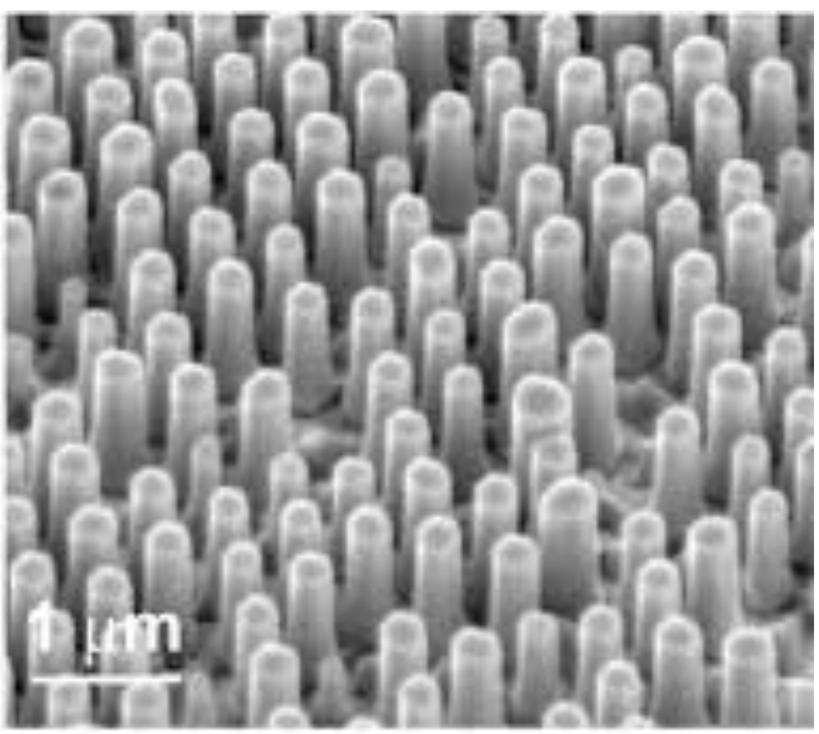

1 µm

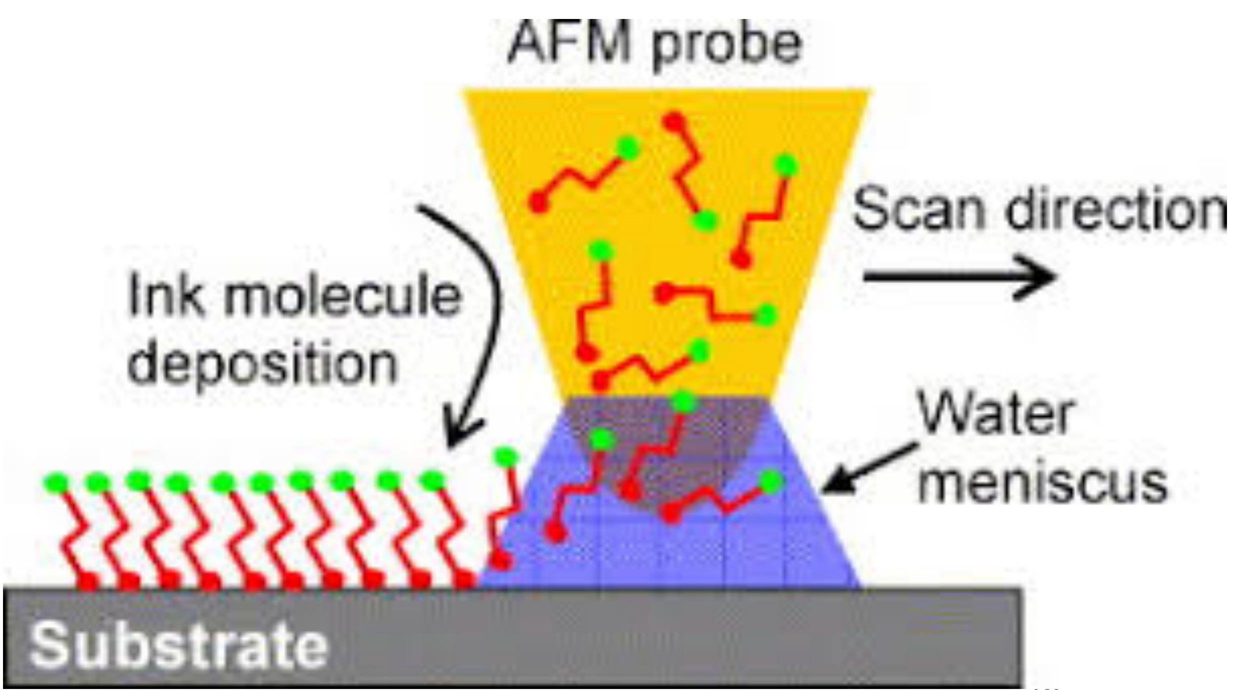

AFM probe
Scan direction
Ink molecule
deposition
Water
meniscus
Substrate

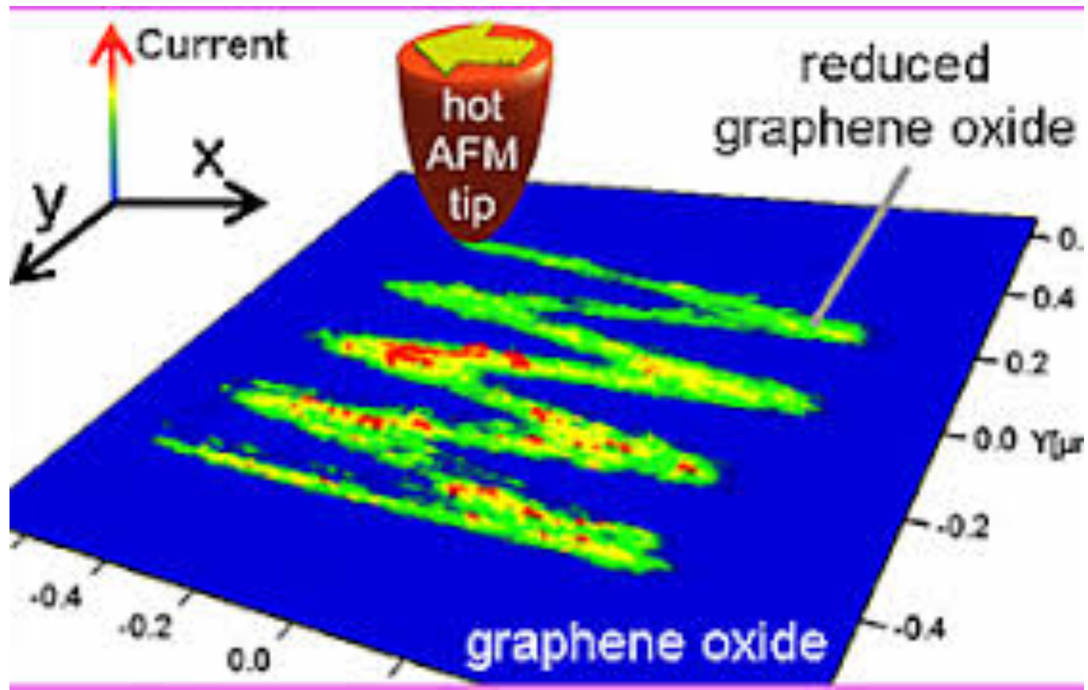
Current
x
y
hot
AFM
tip
reduced
graphene oxide
graphene oxide
0.4
0.2
0.0 Y[μm
-0.2
-0.4
-0.4
-0.2
0.0

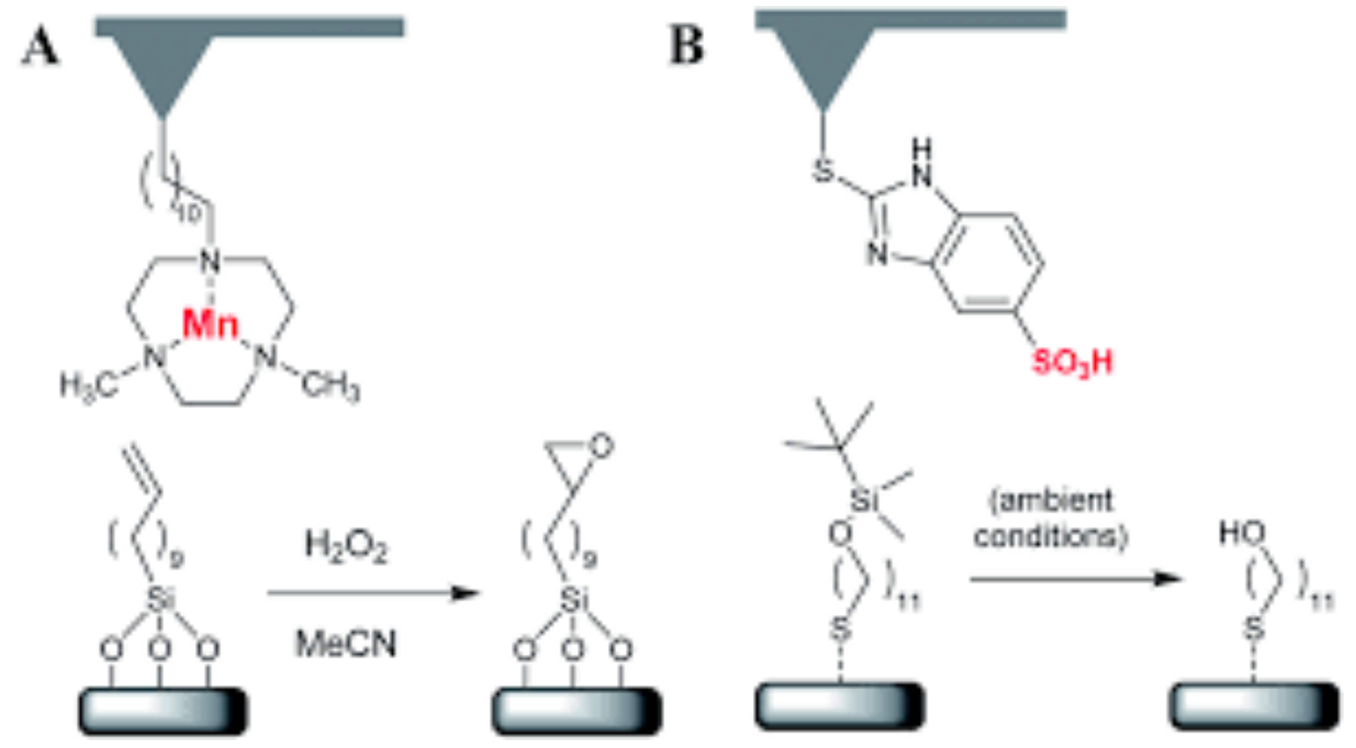
A
B
Mn
H_3C
CH_3
SO_3H
H_2O_2
MeCN
(ambient
conditions)
HO

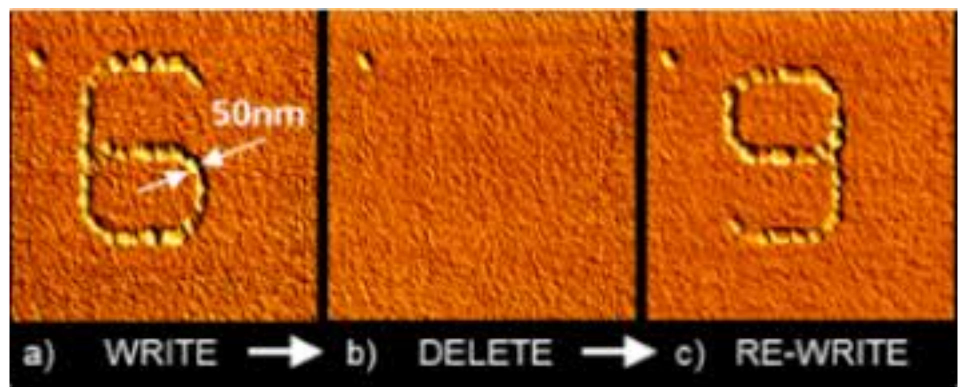
50nm
a) WRITE
b) DELETE
c) RE-WRITE

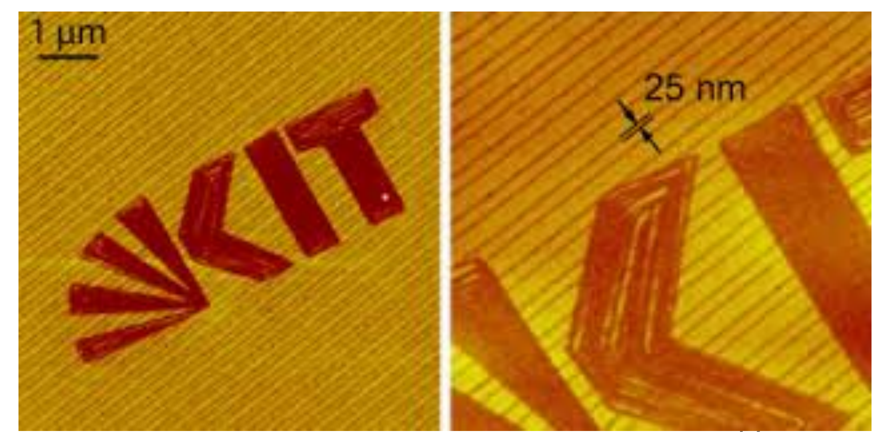
1 μm
25 nm

STM-Based Nanolithography

STM tips typically are atomically sharp and are composed of W, Pt–Rh, or Pt–Ir wires. The tip–surface distance is regulated by feedback electronics to maintain a constant feedback signal (e.g., tunneling current or tip height).

To go beyond imaging to achieve manipulation or fabrication, the targeted molecule or molecules must be broken free from the rest of the surface materials. In other words, local bonds must be weakened or broken.

Experimentally, one can adjust the tip–surface separation, bias voltage, or tunneling current.

The tunneling current depends on the separation distance, following a negative exponential relationship.

In principle, individual molecular manipulation is best achieved using interatomic or intermolecular forces between the tip and surface species. Fabrication involving breaking or formation of chemical bonds is best carried out using tunneling current, which is highly local (e.g., 1 nm or smaller).

Using atomic forces, Eigler and coworkers first demonstrated the precision of STM manipulation at 4 K by advancing an STM tip to the very close proximity of the surface atoms or small molecules.

The overlap of the wave function between the tip and surface species resulted in strong interatomic or intermolecular interactions between the tip and the selected atom or molecule.

The tip can then slide or pick up the atoms or molecules and move them one-by-one to the designated locations.

The atoms that were successfully moved by STM tips included Cu, Fe, Xe, Co, and the small molecules included CO and O_2.

These artificially engineered structures provide a unique opportunity for observation and investigation of size-dependent quantum behavior such as quantum corrals and quantum mirages.

Larger molecules such as porphyrins have also been positioned by Jung*et al.* at room temperature.

Tunneling current has been used to induce local chemical reactions: the breaking and formation of bonds. For small molecules, one can understand such processes as placing electrons in the antibonding orbital or removing electrons from the bonding orbital, which cause the breaking of the chemical bonds.

Ho was successful in breaking O-O, and Si-Si bonds on surfaces, as well as in forming C-Fe bonds. Rieder and coworkers combined tunneling current and forces to break C-I bonds, and to direct two phenyl radicals to form diphenyl molecules.

Less localized lithography may also be accomplished by using an STM tip as an electrode to induce local electrochemical reactions such as the oxidation of adsorbates or the substrate itself in the case of conductive or semiconductive materials.

The local electrical field under the tip provides another means of manipulation. During STM imaging, the electrical field typically ranges from to 10^6 to 10^7 V/cm. The field strength may be increased to 10^8 V/cm, which is comparable to the field experienced by valence electrons. Si-Si may be dissociated under high electrical fields.

It is more difficult to understand the manipulation mechanism for large molecules. Nevertheless, successful examples may be found in the literature including porphyrins, and hydrocarbon chains.

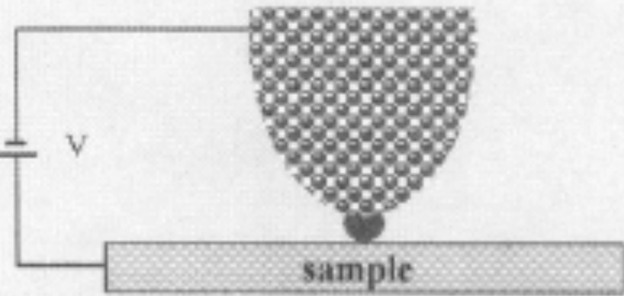

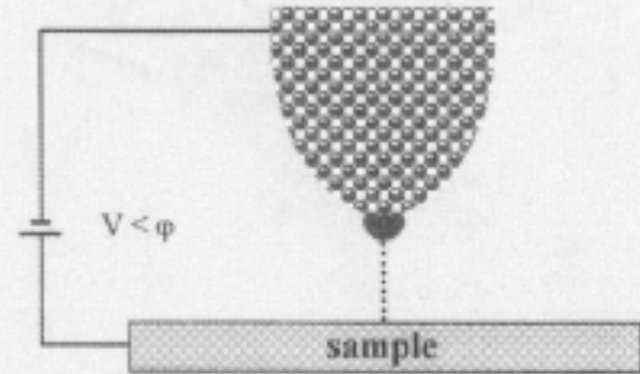

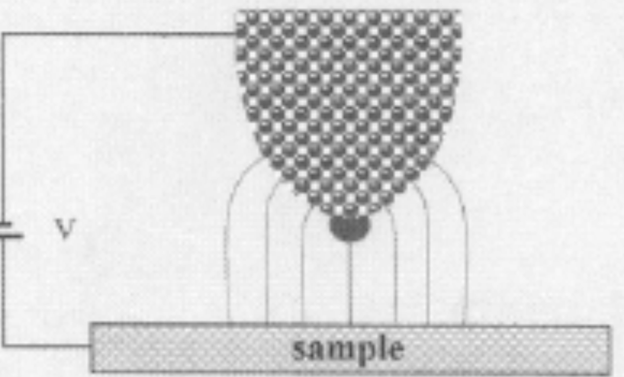

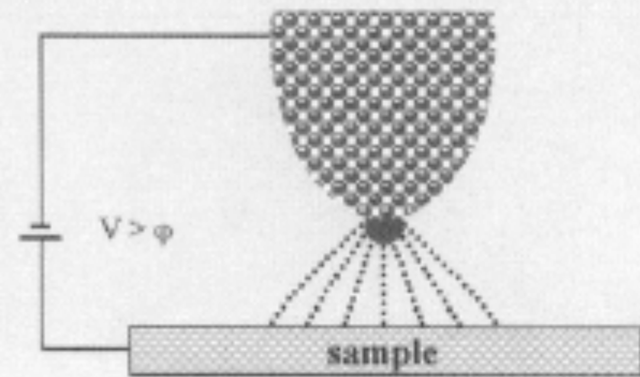

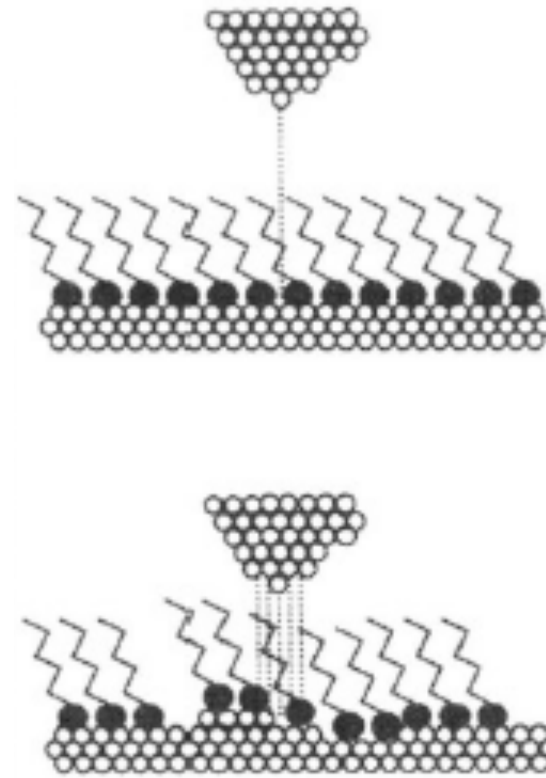

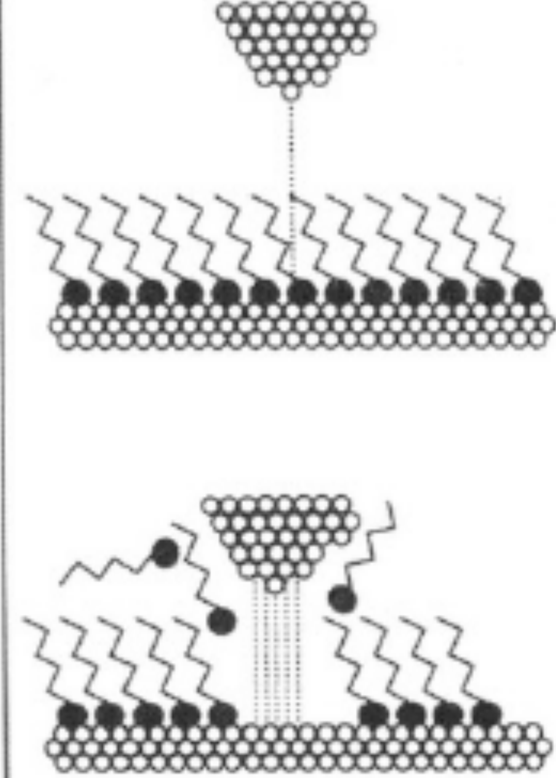

The tunneling electrons broke the sulfur-gold chemisorption and thus caused the thiols to detach.

AFM-Based Nanolithography

AFM-based lithography is a very active area of research because of the flexibility and simplicity of the technique.

AFM tips may be used to carry catalysts to selectively induce surface reactions, or as a pen to attach molecules on surfaces in DPN and its derivative techniques. AFM tips may also be used as an electrode to direct local oxidation on surfaces.

Local force provides another means for AFM fabrication.

AFM-based nanofabrication techniques: nanoshaving, nanografting, nanopen reader and writer (NPRW).

In these methods, the surface structure is first characterized under a very low force or load. Fabrication locations are then selected, normally in flat regions, for example, Au(111) plateau areas. Then nanopatterns are produced under a high force.

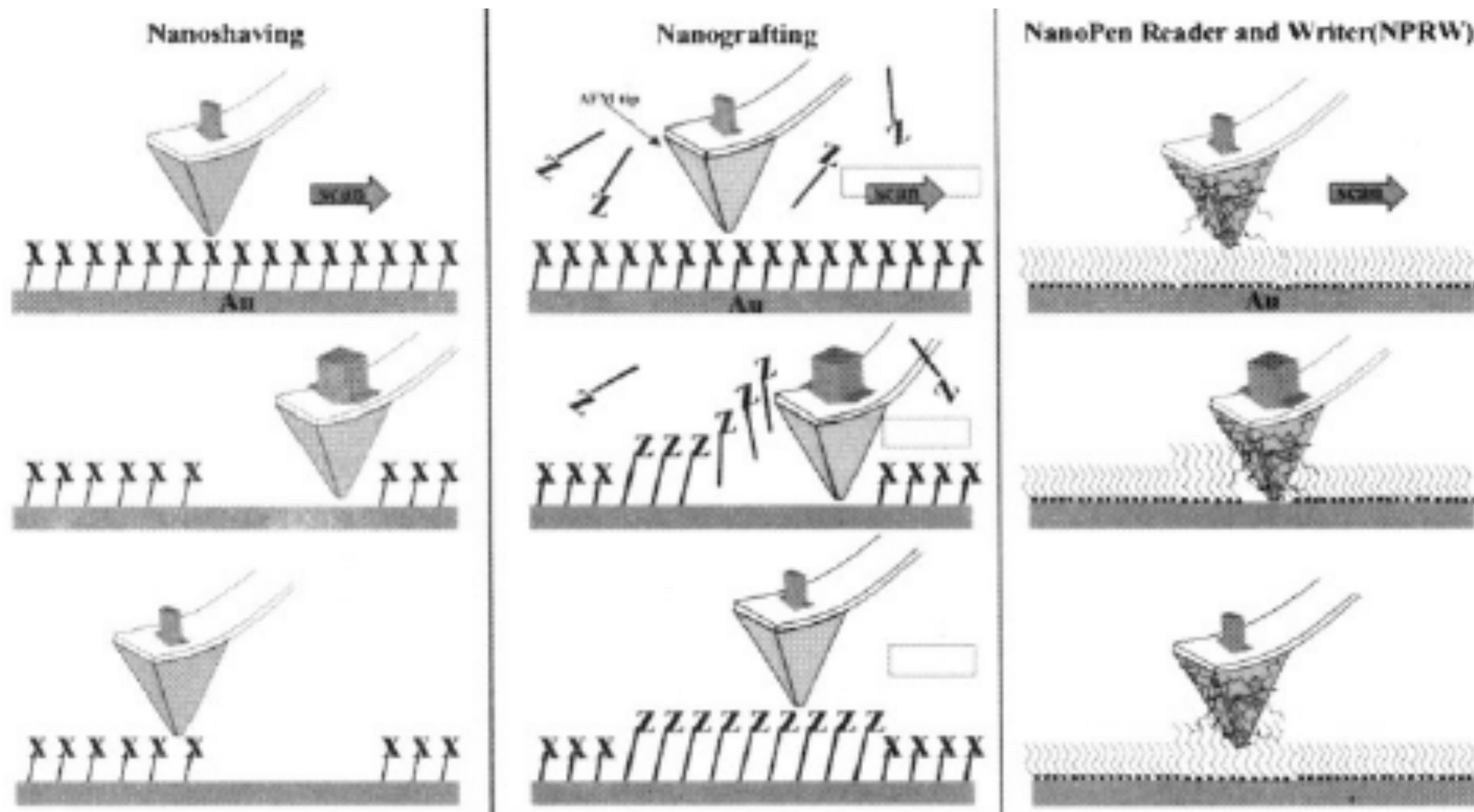

In nanoshaving, the AFM tip exerts a high local pressure at the contact. This pressure results in a high shear force during the scan, which causes the displacement of SAM adsorbates.

In nanografting, the SAM and the AFM cantilever are immersed in a solution containing a different thiol. As the AFM tip plows through the matrix SAM, the thiol molecules in the solution adsorb onto the newly exposed gold surface.

In NPRW, the tip is pre-coated with desired molecules and these molecules are transferred under high force to the exposed substrate. The nanostructures are then characterized at reduced loads.

Compared with other fabrication techniques such as photolithography, and microcontact printing, nanografting and NPRW have several advantages:

First, an edge resolution of 1 nm is routinely obtained.

Second, nanostructures can be characterized *in situ* and with high resolution.

Third, the setup is able to produce complicated patterns automatically. Multiple components can be produced by varying the solution or tip coatings.

Fourth, one can quickly change and/or modify the fabricated patterns *in situ* without changing the mask or repeating the entire fabrication procedure.

Applications of AFM lithography are promising in the areas of nanoelectronics and nanobiotechnology.

Preliminary success in producing nanopatterns of biosystems such as proteins and DNA have been demonstrated. The size of protein patterns ranges from 5 nm to 1 µm. The strategy is to first pattern SAMs using the SPL-based lithography.

These SAM nanostructures serve as templates for subsequent fabrication processes such as patterning proteins by selective adsorption. Selectivity of protein adsorption can be achieved with knowledge of the variation in protein affinity towards different SAMs.

Various nanolithography techniques represent an engineering approach to position molecules in two and three dimensions. The approaches are complementary to the “bottom-up” material synthesis methods, because they provide a means to fabricate ultra-small electronic components, sensing elements, and scaffolds for biomaterial engineering.

There are **pros and cons** among these approaches. Because of the high throughput, X-ray, electron- and ion-beam lithography are, in most situations, the choices of semiconductor industry as the future technology for manufacturing IC and devices. **Soft lithography** such as microcontact printing and nanoimprint provide simpler and less expensive means to produce nanostructures of organic and biological molecules. **Nanoparticle lithography** is specialized in producing periodical arrays of inorganic as well as biological materials.

SPL exhibits the highest spatial precision, and is still a research technique at present. This approach is mostly used to address fundamental scientific issues such as size dependent or quantum properties of selected systems. One concern with SPL is the serial nature of the process and low throughput.

Two approaches are in progress to improve the throughput: automating the nanofabrication, and/or using parallel probes. The unique advantage of spatial precision makes SPL a promising tool for future biotechnology, especially in engineering biochips, sensors, and molecular based devices.

Nanolithography and Nanomanipulation

In the last decades the field of nanolithography has grown extensively and found innovative applications in the area of **nanofabrication**.

The field of nanolithography starts where microlithography stops.

This part mainly include: (a) Templated growth and (b) Scanning probe microscopy (SPM) based lithography such as dip-pen lithography and anodic oxidation.

Electron beam lithography and focused ion beam lithography (FIB) are widely used lithography tools for features with sizes around 40–50 nm
and greater.

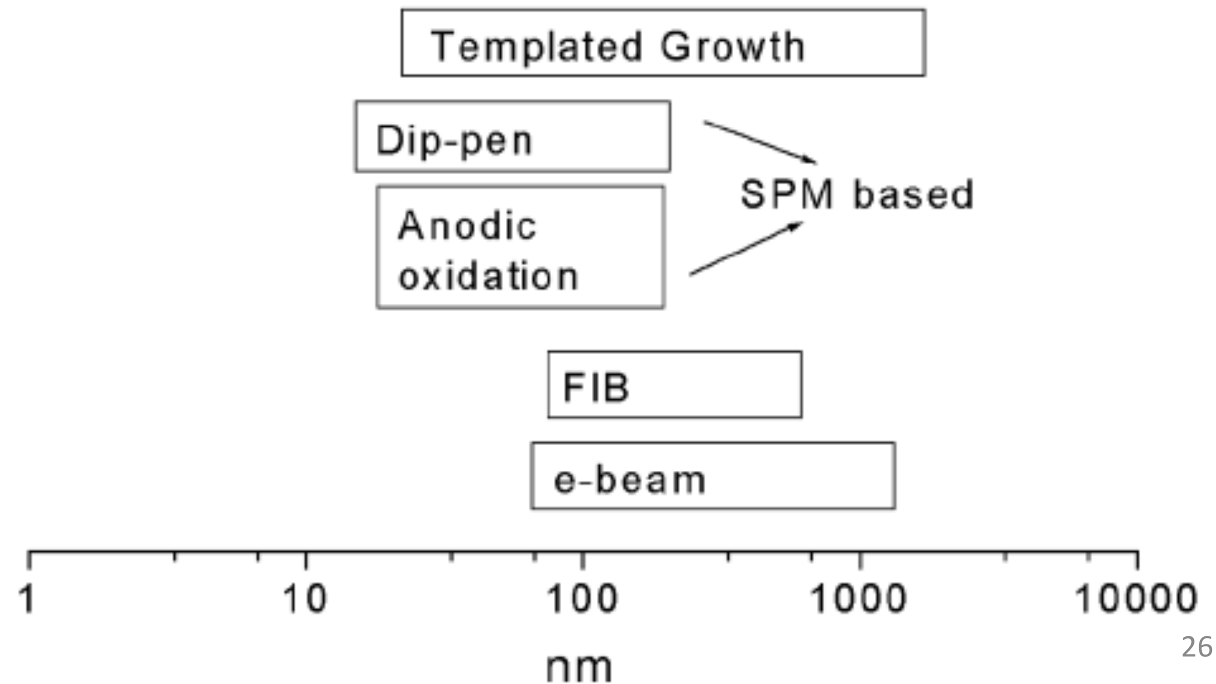

A combination of optical and e-beam lithography provides a step down from the macroworld (@mm) to a length scale of tens to a hundred nanometers.

Nanolithography fabricated objects in the sub 100 nm scale are then manipulated to make contact to electrodes created by an e-beam.

A 100 nm gap has been created on a 500 nm wide line by e-beam lithography which acts as an electrode for NPs and nanowires which can be placed in the gap using nanomanipulation.

Nanolithography and nanomanipulation are the basic tools to provide the bridge to the world of optical and e-beam lithography which interfaces the world of macro-dimensions.

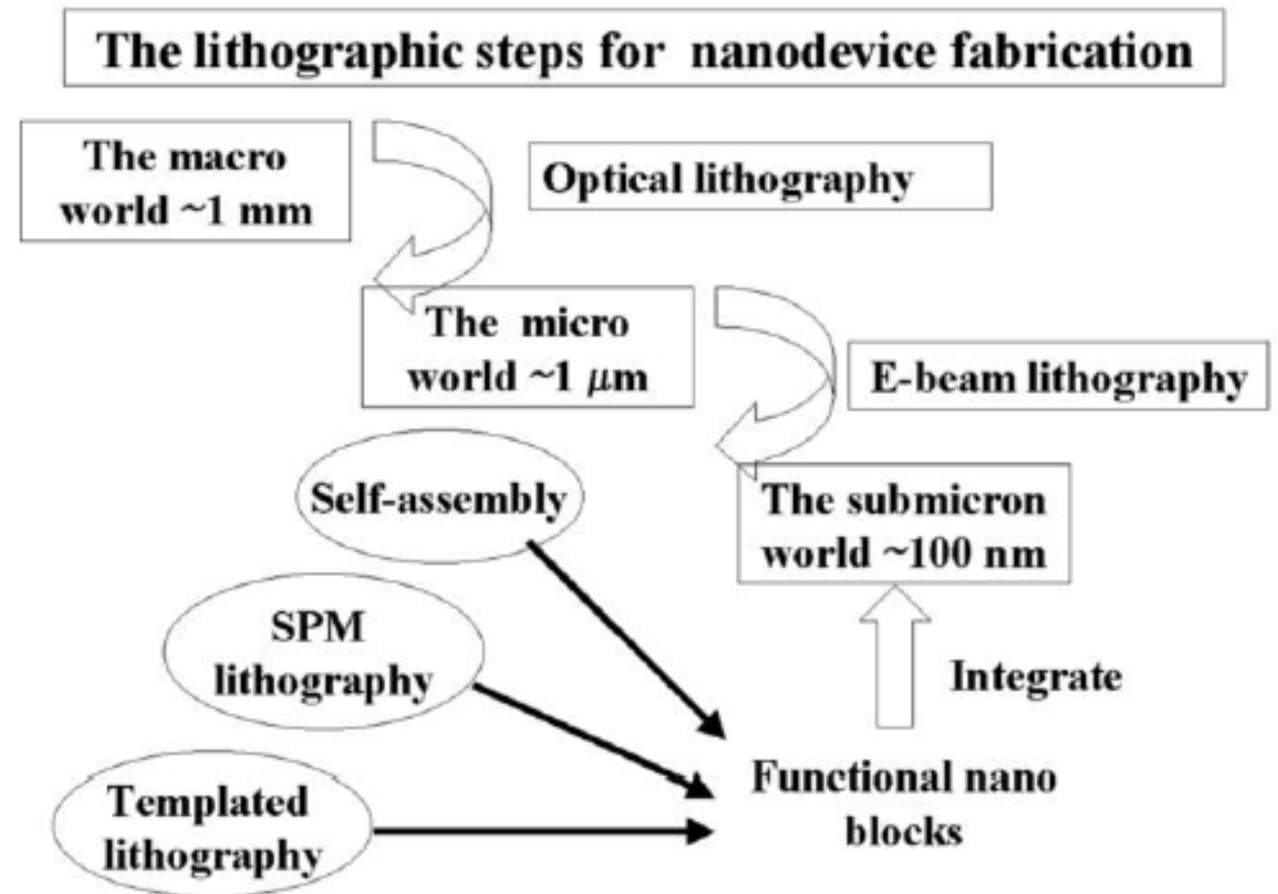

Template Fabrication

One of the most popular and probably the cheapest method of nanolithography is to use nanometer size templates that can be used to fabricate **nanowires**. In some cases this allows fabrication of arrays. This is a chemical route where the nanowires are actually grown by electrodeposition, the sol–gel technique or from the vapor phase.

The advantage of this technique is that one can decouple the fabrication of nanowires and the templates and can have independent control of them.

The templates used for synthesis are either anodized alumina membranes (AM) or etched track polycarbonate or similar polymeric membranes (PM). There are other templates for such deposition, however AM and PM are the most popular.

Ease of fabrication, handling and also commercial availability have made these membranes the main stay of template growth. These templates can be procured from commercial suppliers and can also be tailor-made to a specific use. The templates contain cylindrical pores of diameter as small as 5–10 nm. In some cases the pores form an ordered hexagonal array and the packing density of the pores can be as large as 10^{12}–10^{13} m^{-2}.

Polycarbonate Etched Track Templates

Etched track mica had been used for some time as a template for growth. Etched tracks in PC (polycarbonate), PET (polyethylene terephthalate), PP (polypropylene), PVDF (polyvinylidene fluoride), PI (polyimide) are relatively new and are generally used for preparing high aspect ratio pores in free-standing membranes.

These membranes, which are used as filters, are generally made from high purity polymer films which are exposed in a controlled way to high energy (>1 Mev) charged particles in a nuclear reactor or in a high energy heavy ion accelerator.

When high energy heavy ions of energy more than several hundreds of KeV move through an insulator the electronic energy loss leads to latent track formation. Such tracks can also be produced by using energetic alpha particles in a nuclear reactor using the (n-a) reaction.

During irradiation by swift ions, latent ion tracks are formed along the path of the ions. After irradiation, the material is subjected to chemical treatment leading to formation of the hollow channel from the latent ion track.

The size and shape of the etched ion track is determined by the chemical processing. The etch process depends on (i) the energy deposition density of the ion along its path, on (ii) the radiation sensitivity of the material, on (iii) the storage conditions of the ion-irradiated material before etching, and on (iv) the etchant.

The etching process is generally quantified by the track etch ratio which is the ratio between the track etch rate and the bulk etch rate. The optimum ion type seems to be Kr or Xe ions at specific energies up to about 20 MeV per nucleon.

If the material is stored in oxygen, oxidation of the radicals formed during the irradiation makes the latent ion track susceptible to selective track etching.

Storing at temperatures close to the glass transition temperature of the polymer can enable it to rearrange on a molecular scale and may eventually anneal the ion track.

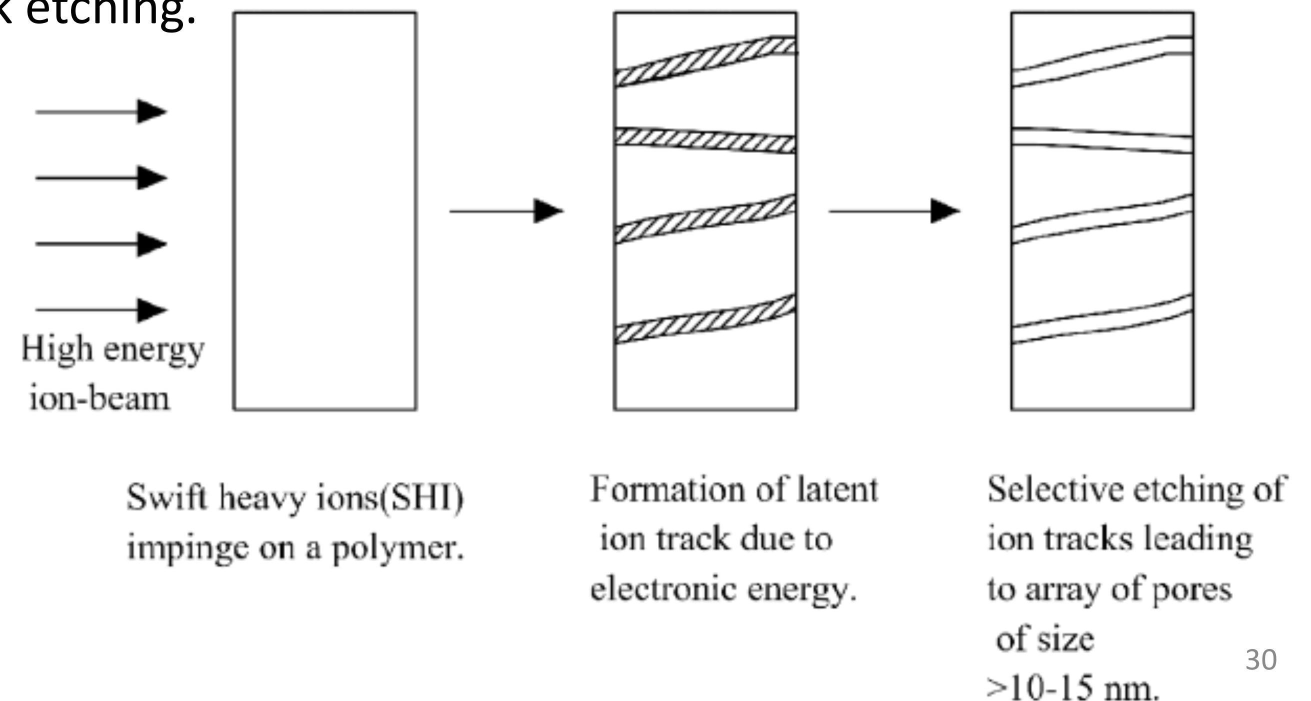

A

1) ion irradiation (parallel, 90° angle)

2) ion-track etching

3) ion irradiation (crossed, 45° angle)

4) ion-track etching

5) metal deposition

electrodeposition

electroless plating

type I

wire / wire architecture

type II

tube / tube architecture

type III

tube / wire architecture

type IV

tube / rod architecture

polymer foil

1)

ion track etching

2)

3)

4)

electroless plating

5)

metal tubes

Illumination, particularly UV radiation (300–400 nm) may lead to photooxidation which increases the track etch ratio by orders of magnitude. Soaking in weak solvents, such as dimethyl formamide or water-soluble gases can sensitize ion tracks in certain polymers.

The requirement for use of these membranes as templates is to have high track etch ratios.

For PC, track etch ratios above ten thousand have been observed.

At the other extreme, addition of solvents, such as methanol, ethanol or propanol can dramatically decrease the track etch ratio, down to 2 to 4 in the case of PET.

Polymers like PMMA are generally etched with an acidic medium leading to very low etch track ratios 1–10.

For polymer polyallyl diglycol carbonate (PADC), the etch-rate values increase nearly fourfold if the polymer is irradiated with 100 Mrad dose of electrons at 2 MeV prior to the heavy ion irradiation. The etch tracks were created by 140 MeV Si ions. Generally the highest density of such pores in these polymers is 10^9 cm^{-2}.

Commercially available membranes are etched polycarbonate or polyester of thickness typically in the range 10 to 30 mm and with pore sizes down to 20 nm.

Fabrication of Anodized Alumina Membrane

A highly ordered structure of nanopores in alumina membranes is made generally by anodic oxidation of high purity aluminum foils. Typical pore sizes are in the range 15–100 nm and the pore density can be as high as 10^{10}–10^{11} cm^{-2}. The highly reproducible nature of the alumina membrane makes it a very useful template for the formation of a number of different types of nanowire.

The alumina membrane can be etched out after growth and this gives rise to free nanowires which can be used for a number of experiments and applications. The growth of porous oxide on aluminum in various electrolytes under anodic bias has been studied for some time.

When aluminum is anodized in certain electrolytes, like phosphoric, sulfuric or oxalic acids, using a two-step process followed by etching, an array of close packed cells (pores) arranged in a near hexagonal pattern develops. Each cell contains a cylindrical pore and the axis of the cell is perpendicular to the surface.

Before anodization, the aluminum foil is de-greased with acetone or trichloroethylene for some time followed by a sodium carbonate wash at around 80 ℃ and vacuum annealed (typically 10-3 Pa) at around 500 ℃ for a few hours. This is followed by an electrochemical polish in acidic solution (like perchloric acid and ethanol mixture or H_3PO_4, H_2SO_4 and CrO_3 mixture).

The anodization process is a two-step process. In the first step the oxidation is carried out in 0.3 M–0.5 M acid medium at temperatures around 5–17 ℃ for 10 to 24 h with applied voltage between 30 and 150 V.

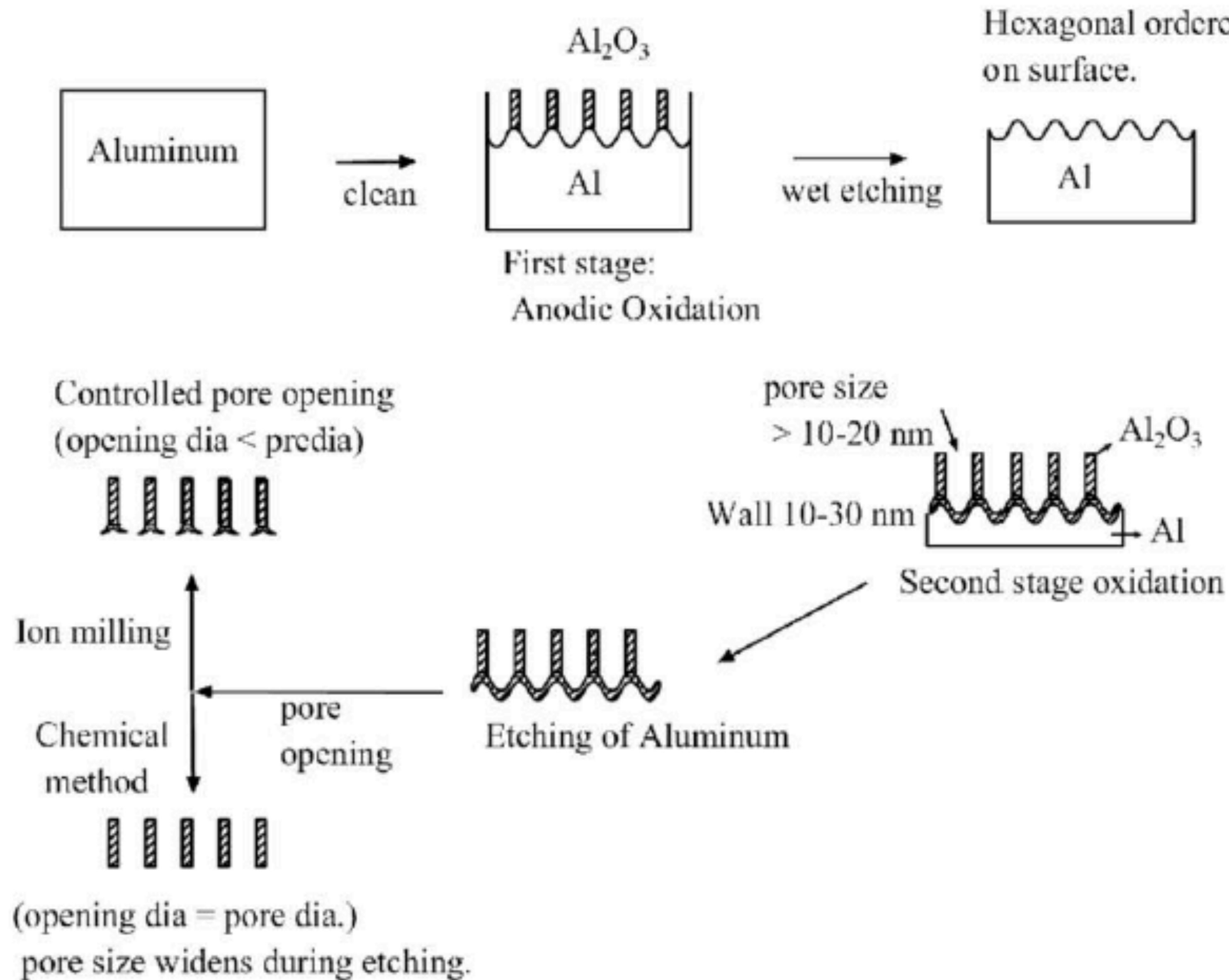

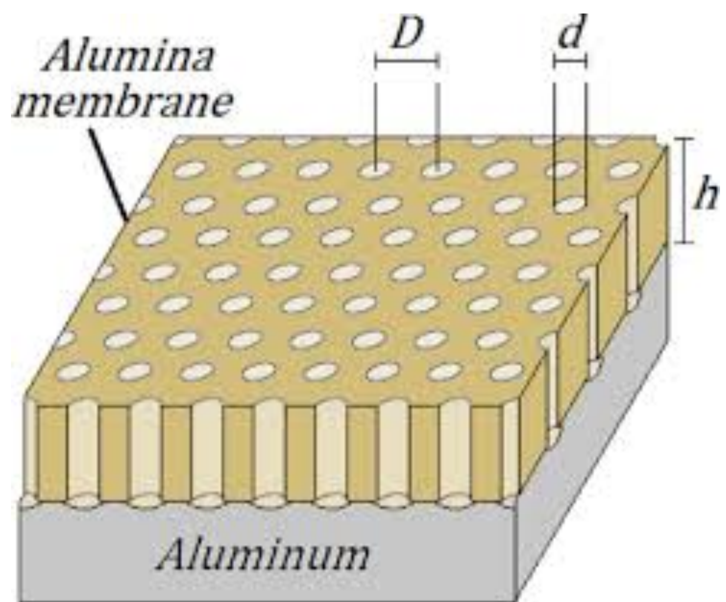
Alumina membrane
D
d
h
Aluminum

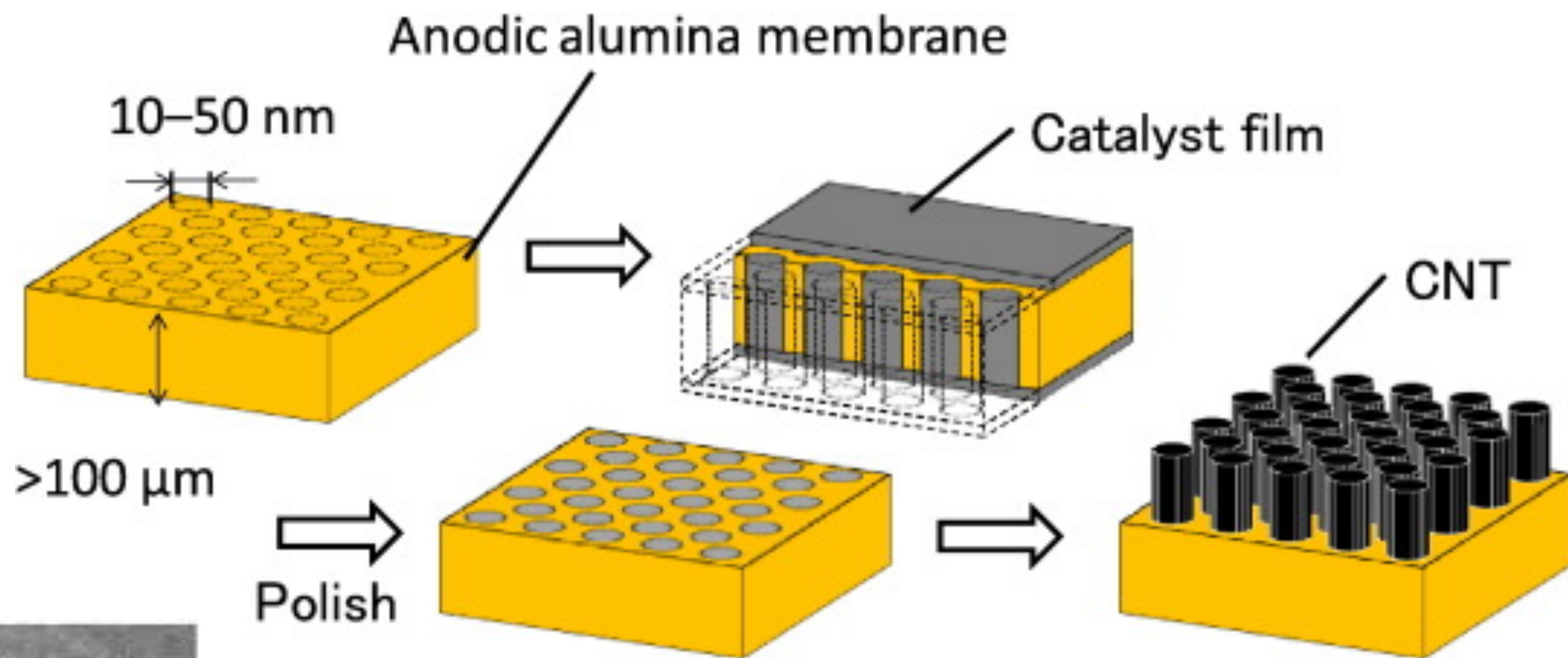
Anodic alumina membrane
10–50 nm
Catalyst film
CNT
>100 µm
Polish

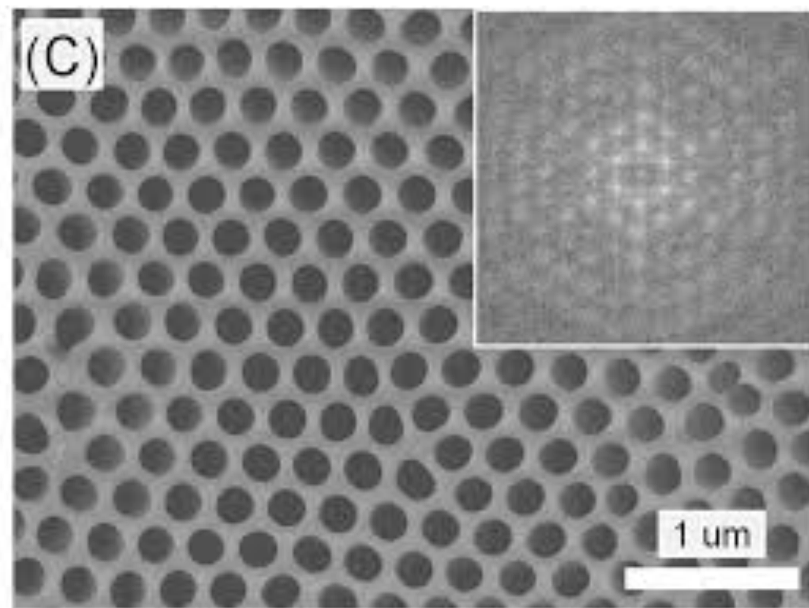
(C)
1 um

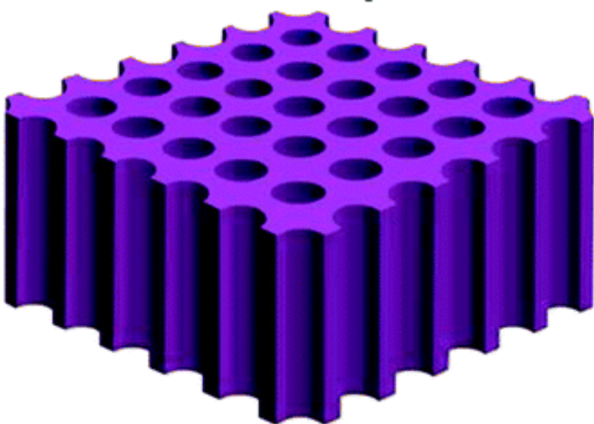
Alumina template
with 200 nm pores
(1)
Solvent
wetting
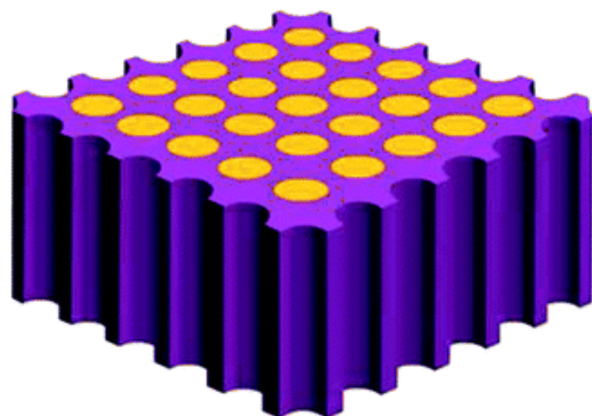
Nanopores filled
with PVDF
(2)
Solvent
annealing
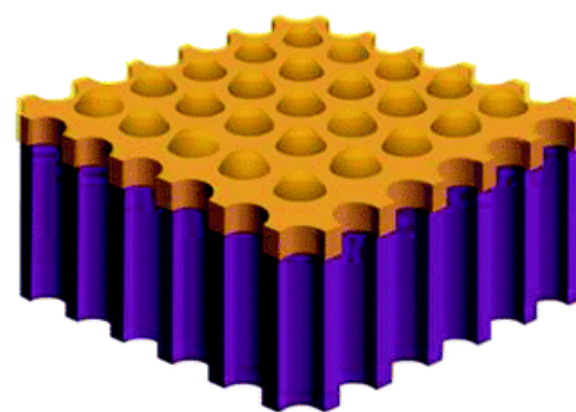
PVDF thin layer formed
by solvent-annealing
(3) Evaporative cooling
water condensation
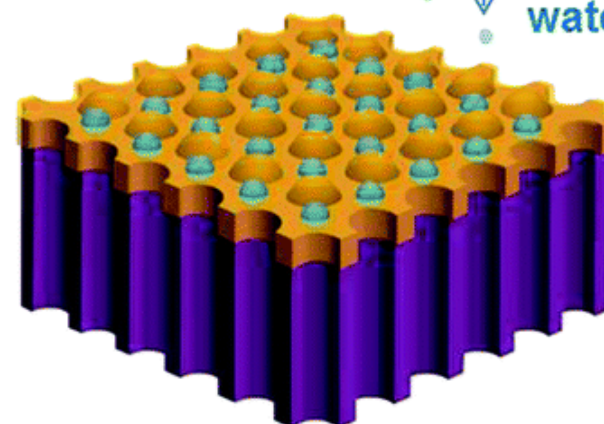
Frost formation
&
its organization on the polymer layer
(4)
Freeze drying
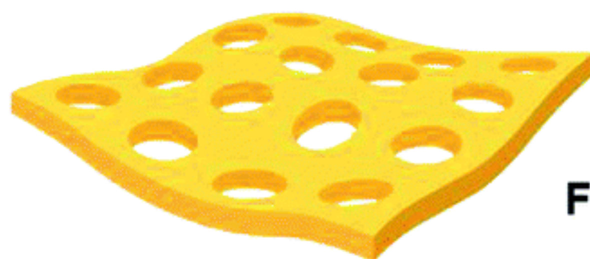
Freestanding
nanoporous membrane

This leads to a layer of Al_2O_3 on the Al foil. This alumina layer is then generally etched with a mixture of orthophosphoric acid and H_2CrO_4 at around 50-60 ℃ for 10-12 h (depending on the oxide thickness). The resulting aluminum has a hexagonal array surface structure. It is then oxidized again in a second step under the same conditions as before. The hexagonal structure that is left behind on the aluminum acts as the template for further growth of the oxide. This leads to typical circular tubes of alumina arranged in a hexagonal array and the bottom of the tube (where it terminates on the aluminum layer) closes on a barrier layer of Al_2O_3 which has a U-shaped structure.

In the next step the Al layer at the bottom is generally removed with $HgCl_2$. This results in a honeycomb of porous alumina with one end closed by a U-tube type structure. The tube runs straight through the thickness of the membrane. The barrier layer at the bottom can be opened chemically or by using ion beams. Chemical methods of removing the bottom layer generally consist of an etch with H_3PO_4, the etching time generally depends on the thickness of the end Al_2O_3. It appears that if this etching is not performed properly it can lead to non-uniform end size. The chemical process of etching the barrier layer also leads to pore radius broadening. The removal of the bottom Al_2O_3 and pore broadening is thus a crucial process.

Recently there has been a report of the use of Ar^+ ion milling (500 eV) to open the bottom cap in the anodized alumina using a normal ion milling machine. The rate of milling can be controlled by the ion beam current density (generally less than 1 mA cm^{-2}) and also the incident angle. The nominal milling rate is 100 A˚ min^{-1} at normal incidence for a current density of 1 mA cm^{-2}.

There are also reports of opening the barrier layer by anodic dissolution. An applied voltage less than the anodic oxidation voltage (@10–20 V) can lead to dissolution of the barrier oxide. For this to happen the dissolution rate has to be more than the anodic oxidation rate. This method is particularly suitable for cases where the alumina is being grown as a template on a substrate and the membrane is thin and supported by a substrate.

The applied bias can control the pore size as well as the pore separation. For growth voltages in the range 30–150 V the pore diameters are in the range 20–150 nm. Typical values are about 1 nm V^{-1} for the pore diameter and 2.5–2.7 nm V^{-1} for the cell spacing. The growth rate depends on the current density and also the temperature. Typical current density is in the range 1–10 mA cm^{-2}.

The growth process is a result of two processes. The oxidation proceeds at the oxide metal interface and there is an electric field assisted chemical dissolution of oxide at the base of each pore. The growth rate is an equilibrium between these growth and dissolution processes.

In general one can get continuous pores over the complete thickness of the membrane. But occasionally one may get damaged pores. Generally the AM films are composed of polycrystalline g-alumina which is expected to have defects. The body of the membrane is more compact and crystalline than the lining of the pore which is more amorphous.

These seem to appear from the oxygen defects (charged) in the Al_2O_3 and thus can be used as a probe to measure the defects in the grown layer. This becomes important when such templates are used for making PL or similar devices.

The two-stage anodization process for making the AM is necessary to produce a hexagonal pattern on the alumina for the oxidation in the second stage. In fact any patterning of the aluminum can act as a template for the oxidation and can produce the template. This has been shown by making a hexagonal array structure on aluminum film by nano-indentation. It was shown that the anodization process leads to growth of hexagonal oxide tubes.

A recent application of the AM is to grow secondary templates of a polymer such as polyaniline. The nanopores have been filled with polyaniline nanowires and even with carbon nanotubes (CNT) grown inside the pores. The polyaniline was deposited by simply immersing the membrane in a solution of aniline and HCl. The aniline was then polymerized at room temperature following usual methods. The secondary templates, such as aligned CNTs, were generated in the alumina nanotubes by the catalytic pyrolysis of acetylene. These secondary templates, which have pores of much smaller diameter, are then used to grow new materials.

The desired material, such as metal nanowires can be introduced into the aligned carbon nanotubes by methods such as electrodeposition. This leads to nanowires with a core structure, such as a Ni wire in a carbon nanotube.

Anodized Alumina Membrane as a Mask for Physical Vapor Deposition

A very important recent application is to use aluminized membranes as a mask for physical vapor deposition. In these cases the membrane is either attached to the substrate or a film of aluminum (typically a few microns thick) is grown on a substrate such as Si. This is followed by the anodic oxidation process to convert the aluminum film to an anodized template. The growth process is either physical vapor deposition or CVD or the membrane is used for reactive ion etching to transfer the mask to the substrate.

Highly ordered arrays of quantum dots of GaAs and InGaAs with narrow dot size distribution, have been grown on GaAs substrates using AM templates.

The templates are prepared by the two-step anodic oxidation. A lift-off process is used to separate thin templates from the aluminum substrates by etching away the unoxidized aluminum foil in a saturated $HgCl_2$ solution. An etch with H_3PO_4 was used to remove the oxide barrier at the end as well as to widen the pores to around 80 nm.

The templates were bonded directly onto the GaAs substrate using van der Waals bonding.

60 nm size magnetic Fe nanodots were fabricated by e-beam evaporation over a 1 cm area of MgO substrate using an alumina membrane (thickness 300 nm, pore density 10^{12} m^{-2}) as a shadow mask on a MgO substrate. The membrane was subsequently removed in a 10% NaOH solution.

Templates Made in Block Copolymers

Spontaneous pattern formation in diblock copolymers has been used to produce a high density (10^{13} m^{-2}) of uniform pores with diameter (10–30 nm) as wide area templates for deposition or synthesis of nanowires, NPs or even a mask for ion milling or reactive ion etching (RIE).
In diblock copolymers different chains or blocks of polymers are covalently bonded. However, incompatibility between two blocks leads to spontaneous self-assembly when they are heated above the glass transition temperature of both.

Template formation by the block copolymer route has certain advantages over the alumina templates.
It is easier to achieve a large density, close to 10^{13}–10^{14} m^{-2} which in the case of the AM is around 10^{12} m^{-2} in most cases.
AM is a two-step oxidation process whereas this is more or less a single-step process. A lower pore size (10 nm) is achievable.
In the case of AM the process of opening up the oxide barrier at the end of the oxidized membrane leads to increase in the pore size. However, in materials fabrication where the processing temperatures go beyond 150 °C to 170 °C these templates become unusable.

In the case of AM a much higher processing temperature (500 °C) is possible. This is a particular necessity where complex functional materials are synthesized in the templates.

Typical copolymer blends are PS (polystyrene)–PMMA (polymethylmethacrylate), PS–PB (polybutadiene) and PS–PI (polyisoprene). Generally the PS is the majority phase that makes the matrix and the other polymer is the minority phase which forms the ordered structure.

The majority PS phase generally has a large molecular weight compared to the minority phase.

The pattern formed depends on the relative chain lengths and the segmental interactions.

As an example the PS–PB block copolymers produce hexagonally ordered PB cylinders in a PS matrix, while in PS–PI one obtains spheres of PI.

For templates and etching masks that use a spherical particle one may restrict the film thickness to around the diameter of the particle (monolayer) to get ordered structures. In the PS–PMMA system one can obtain aligned cylinders of PMMA in PS if an electric field is applied during the curing process. In this case one can get templates with sizes of the order of a micron.

Generally the block copolymer is spin-coated onto the substrate on which the pattern has to be grown or transferred. Some times the wetting of the substrate by the constituent homopolymer components can be controlled by a layer (5 nm) of neutral brush layer of hydroxy-terminated random copolymer of the same constituents.

The curing is carried out at a temperature above the glass transition temperature T_g of both polymers.

The etching of the pattern generally involves a chemical treatment that either stabilizes the matrix polymer or the separated phases against chemical or dry etching.

As an example, with UV exposure and sonication in glacial acetic acid and deionized water the PMMS phase is degraded and can be removed.

Similarly ozonization attacks the carbon double bond in PB which thus can be degraded for preferential etching.

Diblock Co-polymers in solvent(A & B)

Spin coat and heat above T_g of both polymers

Self assembeled pattern formation.

A B

UV degradation
Chemical etching

Electric field induced pattern formation.

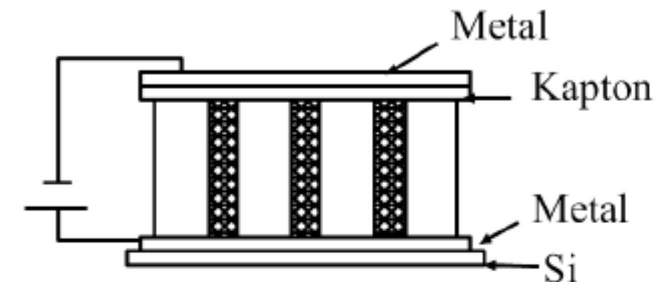

Fabrication of Nanostructures in the Templates

Making templates of ordered nanopores is the starting point for template-based nanolithography.

The next step involves ‘‘filling the pores’’ of the membrane with different materials of interest using one or more available methods.

The methods include electrochemical deposition (ED), vapor phase deposition such as chemical vapor deposition (CVD), pressure injection of molten metals and sol–gel methods.

Methods of deposition in the nanopores:

The chemical routes that are followed depend on the material to be deposited.

In the case of metals or oxides that can be made easily by oxidizing the metal, the most popular route is electrochemical deposition.

For more complex materials like functional oxides a sol–gel method is often used.

For materials like GaN or carbon nanotubes the preferred method is CVD.

Electrodeposition

Electrodeposition of metal inside the nanopores of a membrane is generally performed in baths containing metal salts. The baths are either acidic or basic and use a three-terminal potentiostat. The deposition of nanowires in the porous membranes can thus depend on the knowledge base available for the deposition process.

The thermal diffusion of the ions from the opening of the pore to the interface of the deposition become important.

Generally for ED one needs a cathode where the metal is deposited. For this, generally, one end of the porous membrane is metallized with Au or Ag to a thickness of 500 nm or more by sputtering or evaporation.

With the metallized membrane as the cathode (the working electrode), the counter electrode (anode) is graphite or Pt and Ag/AgCl or calomel forms the reference electrode.

The deposition can be DC or pulsed deposition. The deposition conditions are varied to produce single crystalline or polycrystalline nanowires.

One of the interesting aspect of ED is the deposition of metallic bilayers or multilayer structures from the same bath by changing the bias and adjusting the relative concentration of the two ions.

For instance, multilayers of two metals are often deposited from the same bath by keeping the concentration of the more noble metal (that needs less bias for deposition) very low. At high bias, which is needed to grow the less noble metal, the deposition of the more noble metal becomes diffusion limited due to its low concentration.

One of the earliest studies of Au nanowire (diameter 8 nm) fabricated by electrodeposition in a 5 mm thick etched track mica was reported in 1986. Effect of weak-localization and electron–electron interaction was studied down to 0.3 K.

Co and Cu multilayer wire (40 nm diameter) has been grown in track etched polycarbonate membrane from a Co and Cu sulfate acidic bath using different voltage pulses. The bath compositions were 1 mM of $CuSO_4.5H_2O$ and 0.5 M $CoSO_4.7H_2O$. A voltage pulse of V_{cu}=-0.2 V was used for Cu and a pulse of V_{co}=-0.9 V was used to deposit Co. Evaporated Cu on one side of the membrane acted as the cathode for growth.

These multilayer nanowires were investigated for their giant magnetoresistance (GMR) properties. Around 15% magnetoresistance (MR) was observed at room temperatures in a field of about 0.4 T. Multilayer nanowires of Cu and Co as well as alloy multilayer ((Ni-Fe)/Cu) nanowires have been grown in 6 mm thick polycarbonate membranes using an acidic sulfate bath (using 0.1 M boric acid H_3BO_3 as one of the components).

Pore filling by electrodeposition.

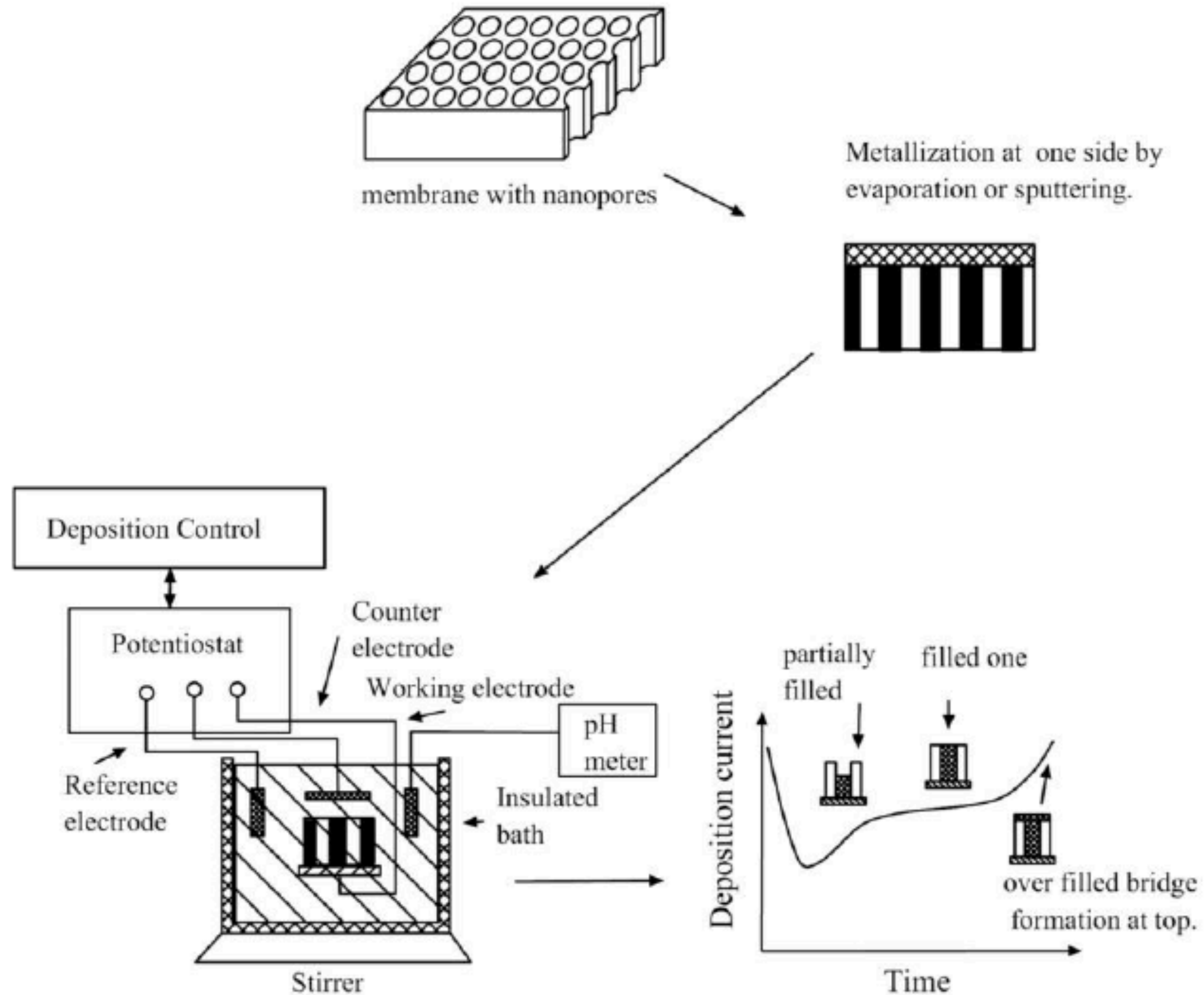

Sol–Gel Method

The sol–gel method is a low temperature synthesis route for complex oxides. It can be used to make complex functional oxide nanowires inside the pores of templates.

In addition to the sol–gel method precursor-based solution deposition routes can also be used for nanostructure formation.

In both cases a postdeposition high temperature anneal (> 500–600 ℃) is needed to form the required stoichiometric phase. Due to the requirement of a high temperature anneal, alumina templates are used as the polycarbonate membranes decompose at a much lower temperature.

For chemical solution deposition the membrane is dipped directly into the precursor solution. For sol–gel growth generally the required sol is prepared and the template is put into the sol for a required period (e.g. 0.5–1 h).

After removing the membrane from the sol it is dried and then annealed at higher temperature before the required phase is formed.

The sol–gel technique is a powerful approach for preparing multicomponent inorganic materials as it is possible to precisely control the molecular microstructure, stoichiometry, high purity, and all at relatively low processing temperatures.

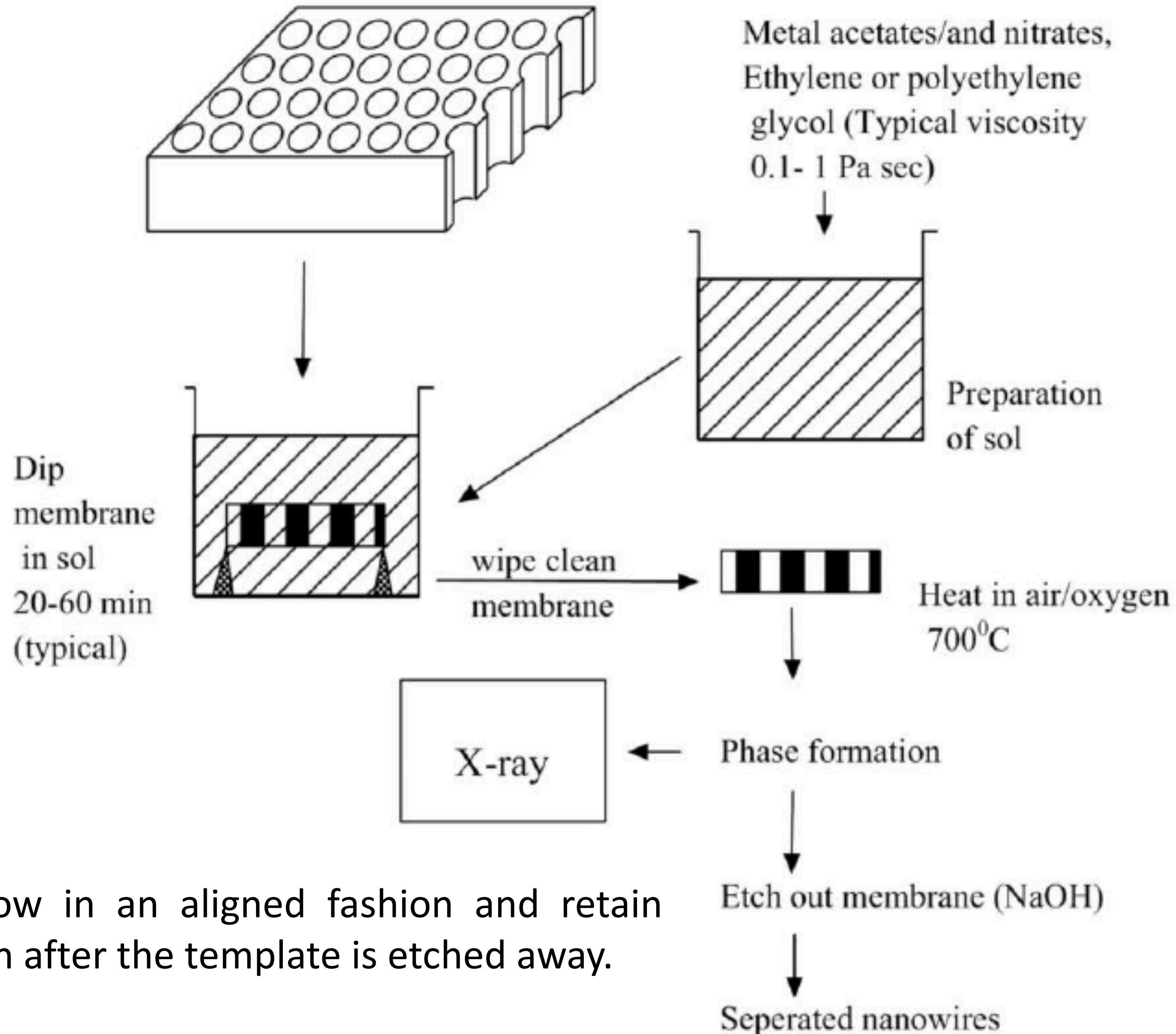

The nanowires grow in an aligned fashion and retain their structure even after the template is etched away.

The sol–gel method has been used to fabricate highly ordered single crystalline anatase phase TiO_2 nanowire arrays in anodic alumina membranes. The wires have an average uniform diameter of around 60 nm and length 25 mm. These wires have broad band visible PL at about 425, 465, and 525 nm that is attributed to self-trapped excitons, and oxygen defect centers.

The TiO_2 nanowires were fabricated using TiO_2 sol made from alkoxide solution prepared by mixing tetrabutyl titanate, ethanol and CH_3COOH. The templates were immersed in the sol. The template was then allowed to dry at somewhat elevated temperature for the sol–gel transition to occur. The final phase formation occurs after heating to above 600 ℃.

Nanowires of 60–200 nm anatase TiO_2 were fabricated using liquid phase deposition in a track etched membrane. The acidic precursor solution used was $(NH_4)_2TiF_6$ (0.2 M) and H_3BO_3 (0.1 M) and was adjusted to a pH of around 1.4 with 1:1 ammonia solution.

Arrays of concentric composite nanowires of ZrO_2 with Co cores were made in an alumina template by the sol–gel method from ZrO_2 sol.

$LiNiO_2$ nanowires in alumina templates have been fabricated. Highly ordered $LiNi_{0.5}Mn_{0.5}O_2$ nanowires were fabricated from sol made from metal acetate cationic sources, citric acid and ethylene glycol.

CVD Method

Templates have been used for the growth of semiconductor nanotubes, including ordered arrays of carbon nanotubes, by chemical and physical vapor deposition.

Aligned CNT with a diameter of about few nm with sufficient graphitic character were made by chemical vapor decomposition (CVD) using propylene gas. The CNTs were made with Fe and Co catalysts or without catalysts.

The CVD process was carried out in a three-zone furnace with deposition temperatures varying from 500 to 1000 ℃. The different temperatures of fabrication yielded different graphitic content with progressive increase in metallic appearance, decrease in resistance and enhanced tube wall structure at high temperatures. However, the graphitic content saturated at a deposition temperature of 800 ℃.

A recent paper reports the synthesis and magnetic behavior of Ni filled CNT. Ni was electrodeposited within the pores of the CNT from an acidic bath of nickel sulfate. The wires with diameter of around 180 nm were found to have a strong uniaxial magnetic anisotropy with easy axis parallel to the wire axis. The parallel coercivity was as high as 185 Oe and much higher than the bulk Ni coercivity of 0.7 Oe.

Pore filling & Nanowire formation using vapor route.

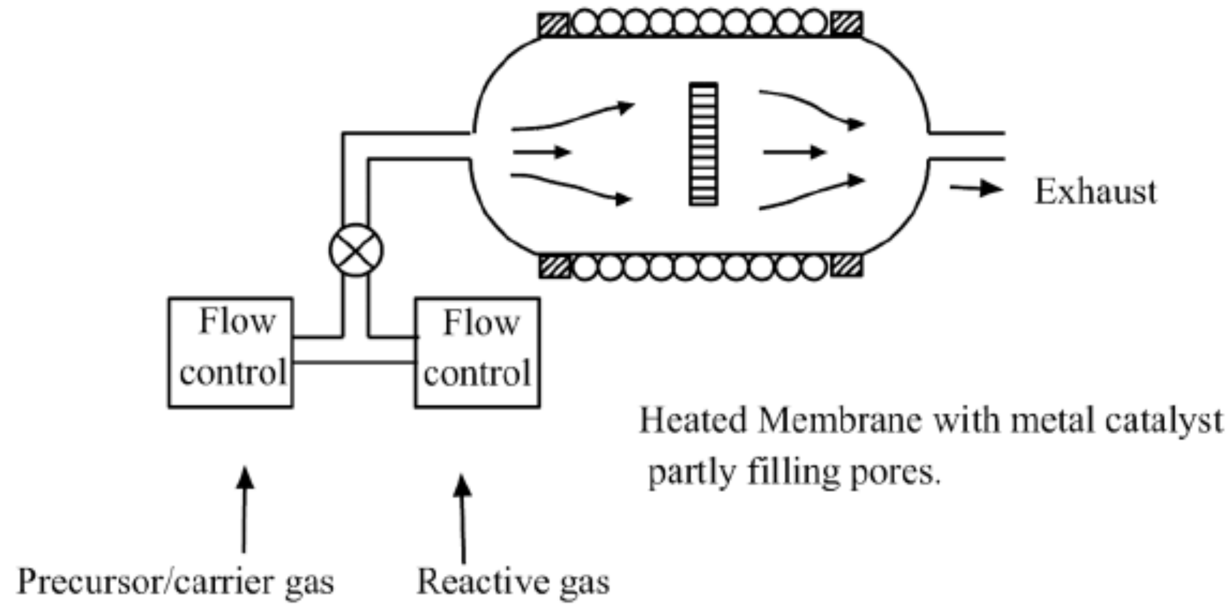

CVD Method

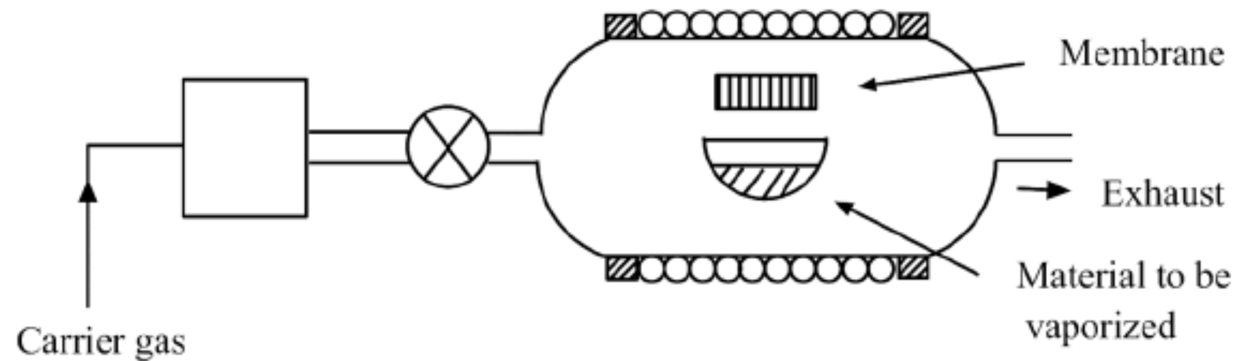

Direct Vapor phase method

Nanowires of GaN have been grown by vapor phase deposition in templates. Single crystalline GaN nanowires (hexagonal wurzite structure) of approximate diameter 14 nm and several micron in length were fabricated in an anodic alumina membrane of around 50 mm thickness.

Aligned carbon nitride nanotubes have been fabricated in an alumina membrane using electron cyclotron resonance (ECR) plasma-assisted CVD of C_2H_2. The membranes have a thickness of 50–80 mm and pore diameter of 250 nm. To promote the flow of ionic fluxes through the nanochannels of the alumina template, a negative dc bias voltage was applied to the graphite substrate holder.

Si nanowires have been grown in templates using a direct vapor–liquid–solid route. The wires were grown in a 60 mm thick and 200 nm pore diameter alumina membrane. The growth was carried out using a 5% mixture of SiH_4 in H_2 in an isothermal low-pressure reactor at 500 °C.

Scanning Probe Based Anodic Oxidation as a Tool for the Fabrication of Nanostructures

Scanning probe microscope (SPM), like the scanning tunneling microscope (STM) and the atomic force microscope (AFM) could be used to create structures at the nanometer scale on a surface. It has also been demonstrated that even atoms can be manipulated using an STM.

The field of SPM-based nanolithography is an established procedure to create patterns at nanometer level that can be transferred onto an underlying substrate, just like any other lithography mask in optical or e-beam lithography. This can lead to fabrication of nanoelectronic devices.

The biggest advantage of the SPM-based lithography (despite its low writing speed) is that the same SPM can be used for writing the pattern and to image it after the writing process.

Due to the finite force of contact, a contact-mode AFM (C-AFM) can mechanically modify a surface, particularly a soft surface. This leads to creation of a pattern on the substrate.

There are two ways to create reproducible patterns with nanometer size features on a surface using the ‘‘chemical route’’ and an SPM. They are dip-pen lithography and SPM-based anodic oxidation.

In both these methods the water meniscus that forms between the tip and the substrate plays the central role. In the case of dip-pen nanolithography there is transfer of matter (mostly organic molecules) from tip to substrate through the meniscus. In the case of anodic oxidation the meniscus acts like an electrochemical cell.

A number of surfaces, both metallic and semiconducting, have been patterned using this route. Both STM and conducting probe AFM have been used for this purpose.

The smallest resolution achieved is around 10 nm while in most cases a resolution of 30–40 nm can be achieved by controlling the humidity in which the microscope is being operated. The typical writing speed is 1–10 mm s^{-1}.

This method combines the chemistry of anodic oxidation of a surface with the spatial resolution and scanning capability of an SPM.

SPM based nano-oxidation

The basic idea in SPM lithography based on anodic oxidation is described below.

The tip is placed in close proximity to the substrate as in an STM or a non-contact mode AFM (NC-AFM) while it touches the surface with a contact force of around 1–10 nN in the case of C-AFM.

Generally the writing operation is done in ambient air with a moisture content of more than 50% RH. The atmospheric moisture capillary condenses on the surface of the substrate forming a meniscus. It is the moisture meniscus that is the active electrolytic medium that is used in the anodic oxidation process. The moisture in this case is a ‘‘nano-reaction, vessel’’ for anodic oxidation.

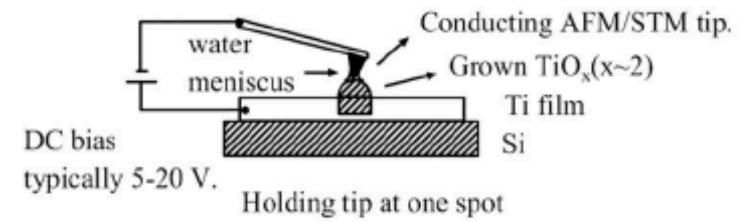

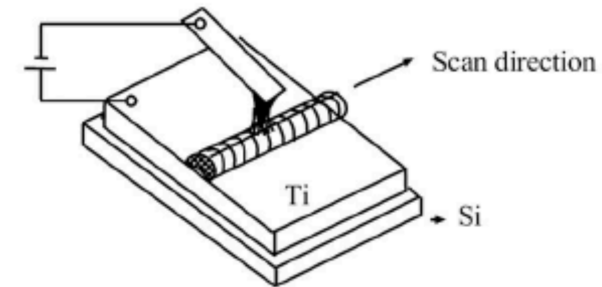

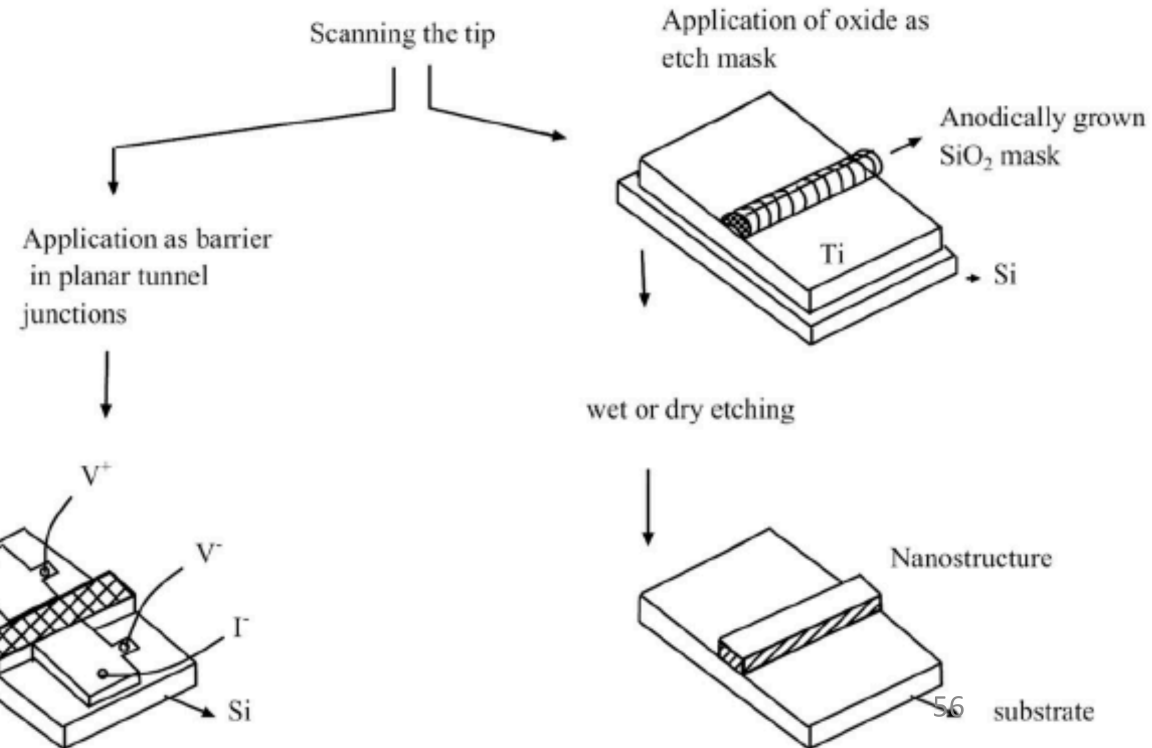

Formation of a meniscus around the SPM tip is one of the important core ideas that are used both in dip-pen lithography and in anodic oxidation. A bias is applied between the tip and the substrate and, for oxidation, the substrate is at a positive bias with respect to the tip.

The oxidation process takes place under an applied field due to the bias and it has to be in excess of 10^7 V cm^{-1} for the oxidation process to begin. The applied field and its magnitude is thus the second important parameter for the oxidation process.

For anodic process: OH^- ions are accelerated to the substrate under the applied field to oxidize the substrate. The mechanism for oxide growth follows the Mott mechanism and the oxide growth rate depends on the electric field at the oxide/substrate interface.

The width and the height of the oxide grown will depend on the applied bias (the higher the applied bias the greater the width and thickness of the grown line). A smaller bias and smaller time of interaction between the field and the substrate will lead to higher resolution.

The radius of curvature of the tip is also important for the anodic oxidation process. Most AFM tips available commercially have a tip radius of curvature of 10 nm.

The nature of the substrate is important for the anodic oxidation process. Two most popular substances are Ti (for formation of TiO_x) and H-passivated Si (for formation of SiO_2).

Oxidation of Metallic Substrates

In the case of the oxidation of a metallic substrate the anodization depends strongly on the humidity of the adsorbed water molecules (as a working electrolyte). The anodization process is carried out in conventional configuration with the tip as the counter electrode and the metal substrate as the working electrode. The anodization takes place when the metallic substrate is biased positively with respect to the tip (STM tip or conducting AFM tip).

Nanofabrication of a Ti surface by the STM tip was carried out using a rather low bias in the range of 3 V and nanostructures with a resolution of 70 nm were produced.

Single atom point contact devices were fabricated with a conducting probe AFM on Al thin films. The Al film (8 nm thick) was grown on a Si substrate with 100 nm SiO_2. The AFM tip was used to make an oxide pattern 500 nm long and 40 nm wide in the middle of a 1 mm wide Al wire. The anodization was done in 10%–20% ambient humidity with a bias of 8-12 V.

In recent years the anodic oxidation has been carried out by using pulsed mode bias on the conducting AFM tip. A room temperature single electron memory was made by this method by growing TiO_x on 2.5 nm Ti film grown on atomically flat α-Al_2O_3. The single electron memory cell showed hysteresis of a memory, even at room temperature. In the pulsed mode one uses a much lower voltage. In pulsed mode while the positive bias of the substrate oxidizes the substrate the negative bias neutralizes the positive space charge from the front end of the growing TiO_x.

Oxidation of Semiconducting Substrates

One of the first reports of single tip SPM-based oxidation of passivated Si (111) was made in 1990. This was followed by reports of oxidation of GaAs and other semiconductor substrates.

A conducting tip AFM (Si_3N_4 tip metallized by 30 nm Ti) was used to make 1–2 nm high and 10–30 nm wide oxide structures on H-passivated n-type Si (100) substrates. The writing was done by contact mode AFM using a contact force of around 100 nN with a cantilever with a force constant of around 0.4 N m^{-1}. The voltage bias used for the writing was in the range 1.5–2.5 eV. The threshold time for oxide formation was found to be around 10^{-4} to 10^{-5} s. The pattern was transferred to the Si substrate below using wet etching with KOH. The oxide grown by the SPM method is stoichiometric SiO_2.

UHV-STM has been used to form oxidation-based nanopatterns on an H-passivated Si (100) surface. Line widths as small as 1.5 nm could be produced. UHV-STM offers a clean way of fabricating much smaller nanostructures of a few nm dimension (as opposed to ten or few tens of nanometer sized features in SPM operating in the air).

Most applications of SPM for nanofabrication were carried out in ambient air. This is presumably due to the ease of operation as well as the cost factor.

Application of non-contact mode AFM in anodic oxidation-based lithography is an important step forward in this field. Noncontact AFM has been used to create feature sizes <30 nm on a 65 nm resist (polymer resist) and was transferred through reactive ion etching (RIE) to the Si substrate (P-doped (100)) on which the resist is coated.

Due to noncontact operation the conducting AFM tip gives out an electron field emission. Typically, the current was in the range of a few tens of pA and it is the emission current that was kept constant by the feedback loop which moves the Z-piezo positioner. The line width written by this method depends on the voltage applied. For a fixed emission current a higher bias will ensure a larger line width due to the geometric effect.

Combination of a pulsed bias and noncontact AFM has been found to improve the control of the writing process. This method reduces the tip–substrate interaction time and thus improves the reliability and lithographic resolution.

The frequency of oscillation and the field pulsing frequencies need to be adjusted to create a definite phase relation between the two and it was found that the minimum line width is obtained when the applied field is on during the time the cantilever tip is furthest from the substrate.

Recent applications of AFM for oxidation include lithography of amorphous chalcogenides such as $GeSb_2Te_4$ films.

Dip Pen Nanolithography

One of the innovative applications of scanning probe microscopy for nanolithography is dip pen nanolithography (DPN). In this special technique the water meniscus formed between the tip and the substrate acts as a medium for molecular transport.

The technique depends on the key phenomenon that the molecule to be deposited on the substrate (which is referred as the ‘‘ink’’) can be transported in a controlled way from the tip (which is initially coated with the ink) to the substrate.

The molecule (the ink) to be deposited on the substrate should interact with the substrate to form a chemical bond, leading to a stable structure. The core concept that the water meniscus at the tip–substrate contact can indeed be controlled and can be used as the molecular transport medium. It was observed that in conditions of low humidity (R_H= 10%–20%) when the tip is in contact with the substrate (and resting on it) the water is transported from the tip to the substrate forming a meniscus.

When the humidity is high (R_H= 90%) for a hydrophilic substrate, there is transport of water from the substrate to the tip around the region of contact, leading to depletion of the water meniscus. For a hydrophobic substrate, for the same high humidity there is transport of water from tip to substrate leading to growth of the water meniscus.

Dip Pen Nanolithography (DPN)

The scan speed of the AFM tip will determine the amount of water that is carried with the tip.

At high scan rates the tip carries less water and the meniscus has less time to grow.

The hydrophobic or hydrophilic nature of the substrate and the scan speed can be used to control the amount of water being transported from the tip to the substrate.

Currently the technique can achieve feature sizes down to 10–15 nm with the capability of using multiple ‘‘ink’’ as well as both serial and parallel writing capability.

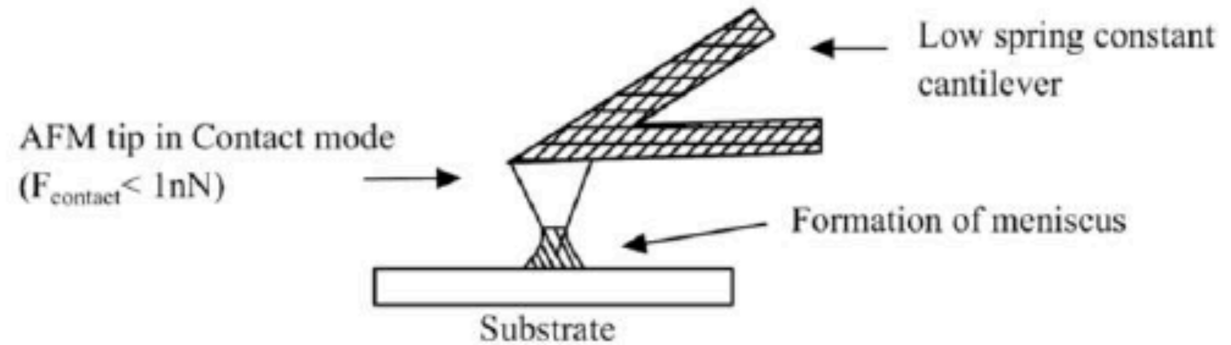

Basic requirements

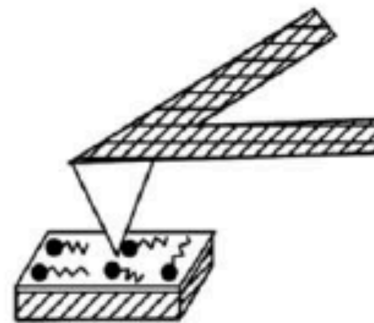

Depositing "ink"on the tip from "ink-pot". A blotting paper soaked in "ink"

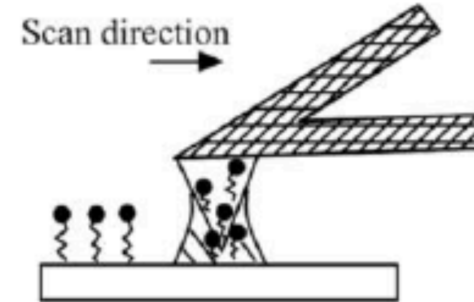

"ink" being transferred from tip to substrate while scanning.

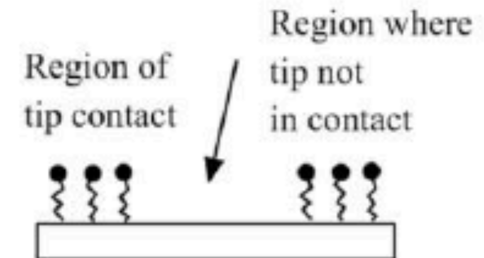

Pattern formation by controlling tip -sample contact.

The patterning in DPN is done by forming a self-assembled monolayer (SAM) of the molecule. The hydrophobic/hydrophilic nature of the SAM becomes an important parameter.

Most of the DPN applications have been done on Au substrates using thiol-based compounds as ink. However, the PDN has also been used to pattern directly on semiconductor surfaces like Si or GaAs. Hexamethyl disilazane (HMDS) was used as the ink and monolayers of HMDS were patterned on the semiconductor surfaces.

The meniscus formed between the tip and the substrate can be an electrochemical cell, by applying a bias between the two, similar to the anodic oxidation using a conducting AFM tip. An electrochemical DPN technique can be used to directly fabricate metal and semiconductor nanostructures.

The application of the bias between the tip and substrate lead to better stability of the structure. The meniscus in this case contains metal salts that can be dissolved in water and it leads to deposition of the metal on the substrate from the meniscus electrolyte by cathodic reduction. As an example 30 nm wide, 0.4 nm high lines of Pt have been drawn on H-passivated P-type Si (100) wafers using 2 wt% H_2PtCl_6 as the electrolyte.

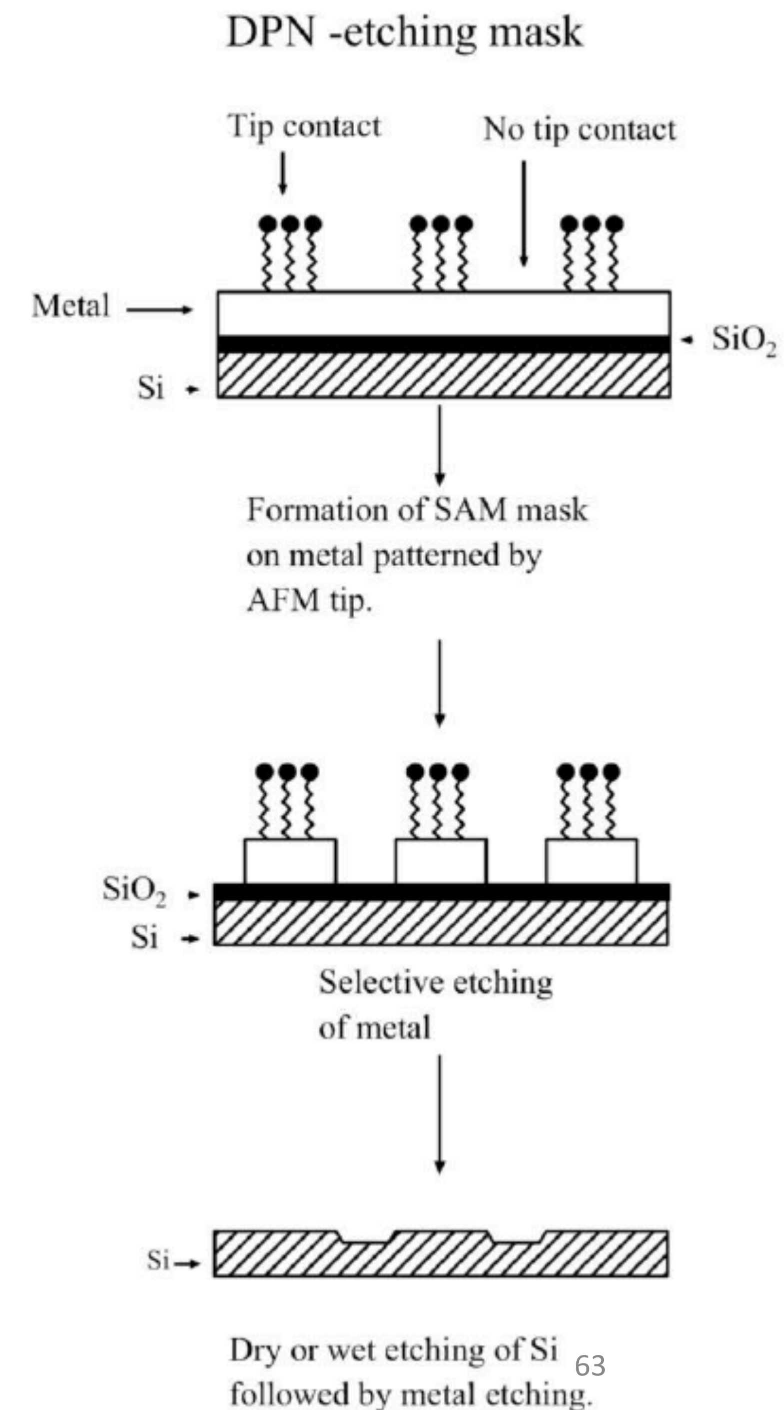

Use of Scanning Probe Microscopy in Nanomanipulation

The field of nanolithography is intimately connected with nanomanipulation. In nanomanipulation generally a preformed nanoparticle, nanotube or a nanowire is manipulated to place it at a predetermined site.

The most widely used tool for nanomanipulation is the cantilever of the AFM that provides a ''robotic'' arm to place the nano-objects in predetermined sites. A nanoparticle weakly adsorbed on a substrate can be moved by an AFM tip when it works in contact mode.

If one wants to place a nanowire between two electrodes an AFM cantilever can be used to image the wire and push it between the two electrodes.

The STM tip can also be used for nanomanipulation. In fact the first atomic level nanomanipulation was done by STM. However, in more recent context, by nanomanipulation we generally imply use of an AFM cantilever to manipulate nano-objects.

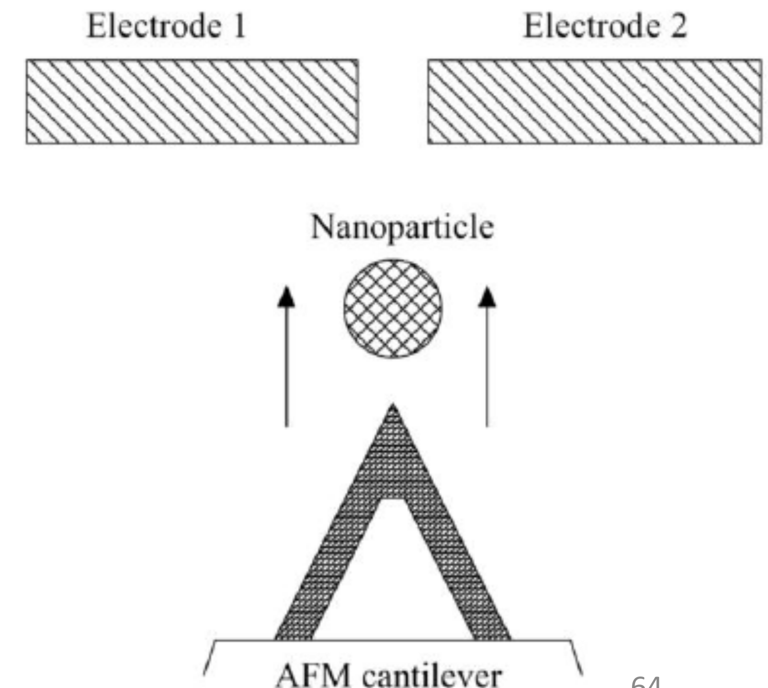

The process of nanomanipulation involves control of a number of forces.

The main two forces are the force of adhesion (F_a^{tp}) between the AFM tip and the adsorbate particle (which will be manipulated) and that between the particle and the substrate (F_a^{ps}).

These forces are mediated by the surface force and depend on the formation of a meniscus on the substrate. While F_a^{ps} stabilizes the particle on the substrate, F_a^{tp} makes the particle stick to the tip.

The contact force between the tip and the particle F_c makes the particle move.

The movement of the cantilever from its equilibrium position and the force constant of the cantilever are determining factors.

Since the experiments are carried out in ambient air, there are capillary forces between the tip and the particle as well as the van der Waal forces between the tip and the particle and between the particle and the substrate.

The balance of these forces determines the final dynamics of the particle movement.

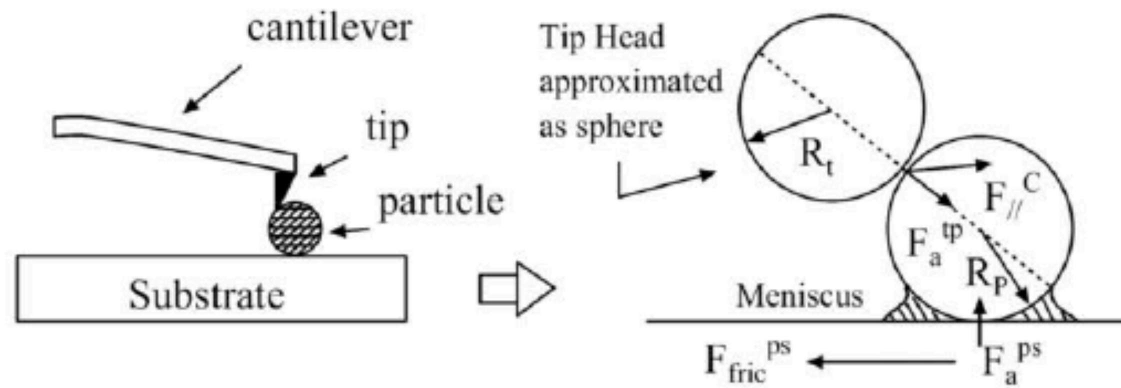
cantilever
tip
particle
Substrate
Tip Head
approximated
as sphere
R_t
$F_{//}^{C}$
F_a^{tp}
R_P
Meniscus
F_{fric}^{ps}
F_a^{ps}
For particle not adhering to tip $F_a^{tp} < F_a^{ps}$
For particle movement on substrate $F_{//}^{C} > F_{fric}^{ps}$
(a)

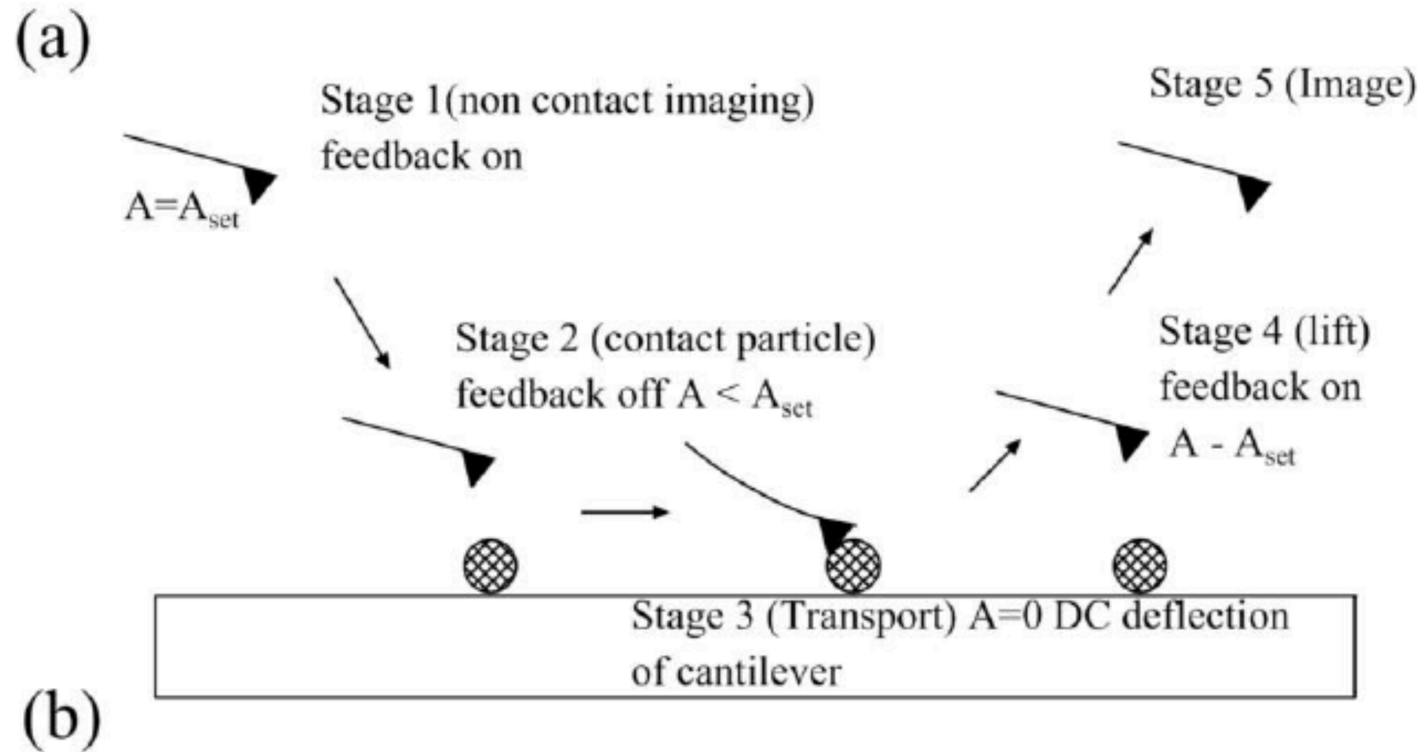
Stage 1(non contact imaging)
feedback on
$A=A_{set}$
Stage 2 (contact particle)
feedback off $A < A_{set}$
Stage 3 (Transport) A=0 DC deflection
of cantilever
Stage 4 (lift)
feedback on
$A - A_{set}$
Stage 5 (Image)
(b)

Nano-Electromechanical Systems

In the past 15 years the field of micro-electromechanical systems (MEMS) has progressed tremendously thanks to the innovative utilization of the techniques of microelectronic fabrication.

In particular, techniques of lithography using optical and electron beams and the development of anisotropic etching (both dry and wet) led to the rapid progress in the field. In recent years there have been new efforts to make mechanical structures of much smaller length scales deep in the submicron range. These efforts have initiated the field of nano-electromechanical systems (NEMS).

The crucial aspect of NEMS fabricated structures is the realization that one is dealing with mechanical vibrations of much higher frequencies. In the case of MEMS the resonance frequencies of the fabricated structures are in the range of tens to hundreds of kHz. For NEMS the frequencies are well into the RF range (1–100 MHz).

Such a high frequency mechanical vibration needs investigation of physical properties (particularly mechanical properties) in a length scale that has not been done previously.

Interestingly, carbon nanotubes, due to their superior mechanical properties and their coupling of size and deformation to electronic structures are an exciting NEMS material.